NASA TECHNICAL MEMORANDUM

NASA TM X-2709

NASA TM X-2709

RESULTS OF URANIUM DIOXIDE - TUNGSTEN IRRADIATION TEST AND POST-TEST EXAMINATION

by John F. Collins, Claude E. deBogdan, and Dominic C. DiIanni

Lewis Research Center
Cleveland, Ohio 44135

NATIONAL AERONAUTICS AND SPACE ADMINISTRATION • WASHINGTON, D. C. • MARCH 1973

1. Report No.	2. Government Accession No.	3. Recipient's Catalog No.
NASA TM X-2709		

4. Title and Subtitle	5. Report Date
RESULTS OF URANIUM DIOXIDE - TUNGSTEN IRRADIATION TEST AND POST-TEST EXAMINATION	March 1973
	6. Performing Organization Code
7. Author(s)	8. Performing Organization Report No.
John F. Collins, Claude E. deBogdan, and Dominic C. DiIanni	E-7083
	10. Work Unit No. 112-27
9. Performing Organization Name and Address Lewis Research Center National Aeronautics and Space Administration Cleveland, Ohio 44135	11. Contract or Grant No.
	13. Type of Report and Period Covered Technical Memorandum
12. Sponsoring Agency Name and Address National Aeronautics and Space Administration Washington, D.C. 20546	14. Sponsoring Agency Code

15. Supplementary Notes

16. Abstract

A uranium dioxide (UO_2) fueled capsule was fabricated by the General Electric Company, Nuclear Thermionic Power Operation (NTPO) and irradiated in the NASA Plum Brook Reactor Facility (PBRF). The capsule consisted of two bulk UO_2 specimens clad with chemically vapor deposited tungsten (CVD W) 0.0762 and 0.1016 cm (0.030- and 0.040-in.) thick, respectively. A central vent tube with a 0.254-cm (0.010-in.) i.d. was attached to the bottom end cap to allow the escape of fission gases. The capsule was operated at a maximum clad temperature of 1690° C and an average flux at the fuel of 0.744×10^{13} nv. The specimen with 0.0762-cm (0.030-in.) thick cladding was removed after 190 hours because of a water leak in the container. The second specimen with 0.1016-cm (0.040-in.) thick cladding was irradiated at temperature for 2607 hours, corresponding to an average burnup of 1.516×10^{20} fissions/cm^3. Postirradiation examination showed distortion in the bottom end cap, failure of the weld joint, and fracture of the central vent tube. Diametral growth was 1.3 percent. No evidence of gross interaction between CVD tungsten or arc-cast tungsten cladding and the UO_2 fuel was observed. Some of the fission gases passed from the fuel cavity to the gas surrounding the fuel specimen via the vent tube and possibly the end-cap weld failure. Whether the UO_2 loss rates through the vent tube were within acceptable limits could not be determined in view of the end-cap weld failure.

17. Key Words (Suggested by Author(s))	18. Distribution Statement
UO_2 fuel CVD tungsten clad Inpile operation, 1690° C	Unclassified - unlimited

19. Security Classif. (of this report)	20. Security Classif. (of this page)	21. No. of Pages	22. Price*
Unclassified	Unclassified	76	$3.00

* For sale by the National Technical Information Service, Springfield, Virginia 22151

CONTENTS

RESULTS OF URANIUM DIOXIDE - TUNGSTEN IRRADIATION TEST AND POST-TEST EXAMINATION

by John F. Collins,* Claude E. deBogdan, and Dominic C. DiIanni

Lewis Research Center

SUMMARY

For inpile operation a fueled capsule containing two bulk uranium dioxide (UO_2) specimens was irradiated in the NASA Plum Brook reactor (PBR). The two bulk UO_2 fuel specimens were clad with chemically vapor deposited tungsten (0.076 and 0.102 cm (30 and 40 mils) thick). Leakage due to a braze joint failure of the 0.076-centimeter specimen was detected during startup. This specimen was removed, and the experiment was completed with the 0.10-centimeter specimen. Irradiation was initiated with a 190-hour fuel redistribution period at 1590° C as the maximum clad temperature.

After redistribution the fuel specimen was thermally cycled between 1690° and 847° C with a 30-minute hold at the maximum temperature. Neutron radiography showed no measurable effect on either the fuel clad or capsule structure. Another set of 24 thermal cycles was run between 1690° and 469° C with a 10-hour hold at the maximum temperature. Radiography showed only slight (0.007 to 0.012 cm, max.) downward dishing of the bottom end cap but no radial swelling of the clad. Results indicate that thermal cycling is not a major cause of the fuel clad swelling under the conditions tested.

Life testing conditions (fission power density, 500 W/cm^3; clad temperature, 1690° C, max.) were maintained for the remaining period up to 2607 hours. Bottom end cap failure occurred some time between 1554 and 2607 hours. Radiography also revealed that the vent tube probably failed during thermal cycling.

The post-test examination was done in the GE-NSP hot cells with the following results: Average thermal fluxes were 1.7×10^{13} and 1.4×10^{12} neutrons per square centimeter per second (>1 MeV). Fission products were deposited throughout the containment can. Forty to sixty percent of the fission gases (Kr, Xe), 0.053 percent of total ^{235}U, and 0.059 percent of total ^{238}U escaped. Maximum swelling was 0.0152 centimeter (0.006 in.) in the clad diameter.

Metallographic examination revealed cracks and weld failures in the cladding, end caps, and central vent. Burnup analysis indicated an average burnup of 1.516×10^{20} fissions per cubic centimeter, based on U^{235} atoms present before irradiation testing.

---

*General Electric Co., Cincinnati, Ohio.

INTRODUCTION

An important consideration in the development of high-temperature nuclear thermionic fuel elements is the suitable selection of fuel and clad materials. The fuel and clad materials must be chemically compatible and dimensionally stable when operating in a nuclear environment at thermionic temperatures. Thus, the properties of these materials in relation to their application must be studied.

Some of the previous work investigated the compatibility between uranium dioxide (UO_2) fuel and two clad materials, tungsten - 25-weight-percent rhenium (refs. 1 and 2) and chemically vapor deposited tungsten (W-25Re and CVD W). These tests were conducted out-of-pile and irradiated in the Plum Brook Reactor (PBR). Results from these tests showed that clad thickness and the method for venting fission gases were not adequate in preventing fuel specimen swelling. As a result, the experiment described in this report was conducted to investigate fuel form stability using tungsten and UO_2. This effort includes the in-pile operation at the PBR and postirradiation examination of a capsule containing two bulk UO_2 - CVD-W clad fuel specimens. The postirradiation disassembly and examination of the capsule was performed in the General Electric-Nuclear Space Propulsion hot cells.

The objective of this experiment (designated as 66-03-2) were to

(1) Study the structural integrity and compatibility of bulk UO_2 fuel and CVD W cladding.

(2) Obtain fission gas release data from bulk UO_2 fuel through a 0.0254-centimeter (0.010-in.) inside-diameter central vent that penetrates the central fuel cavity.

(3) Determine if clad swelling can be reduced by increasing the CVD W clad thickness from 0.0762 to 0.1016 centimeter (0.30 to 0.40 in.). (However, this objective was not achieved because of a leakage of a braze in the 0.0762-cm (0.030-in.) clad specimen capsule.) Determination of thermal cycling effects on clad swelling was substituted in the early testing stage.

(4) Life test the fuel to a burnup of 4×10^{20} fissions per cubic centimeter of UO_2 at a clad temperature of 1690° C.

Experiment 66-03-2 was a fueled lead type of experiment containing specimens representative in size and configuration of a single thermionic cell.

The capsule design, fabrication, and installation is the same as experiment 66-03-1 and was described in reference 4.

DESCRIPTION OF CAPSULE

Capsule Assembly

The clad fuel specimen and capsule illustrated in figure 1 is basically similar in design to that of experiment 66-03-1 (ref. 4) except that a vent tube penetrating the fuel cavity and bottom end cap was added. The fuel cladding was 0.1016-centimeter (0.040-in.) thick CVD W. The top and bottom end caps were arc-melted tungsten, and the thermocouple stem was CVD W-22Re tubing. The vent tube was CVD W. A bottom skirt was made a part of the sleeve cladding to space and hold a niobium target disk with a vent hole off center. This target disk was to trap any UO_2 fuel or condensable fission products lost through the vent tube.

Materials of Fuel-Clad Specimens

All materials used in the fabrication of this fuel specimen were characterized according to GE-NTPO S.I. 231982. Most materials underwent chemical analysis in addition to examination of microstructure, hardness determination, and, for CVD W, an investigation of thermal stability.

Uranium dioxide fuel. - Fuel pellets (0.920-cm (0.362-in.) o.d., 0.318-cm (0.125-in.) i.d., and 1.917 cm (0.755-in.) long, weighing 11.29 g) were fabricated of ceramic grade UO_2. Enriched and natural grades of UO_2 powders were blended in proportions to provide a ^{235}U enrichment of 16.19 percent. This powder blend was dissolved in nitric acid, and ammonium diuranate was precipitated from the uranyl nitrate solution. The ammonium diuranate was filtered, dried in air at 150° C, and then decomposed to fine (0.5 to 5 μm) powder in hydrogen-nitrogen atmosphere at 625° C. This powder was isostatic pressed at 1.723×10^8 newtons per square meter (25 000 psi) to form pellets that were sintered in dry hydrogen at 1680° C for 4 hours to 96 percent of theoretical density.

The sintered pellets were core drilled to a 0.318-centimeter (0.125-in.) inside diameter and then ground to a 0.920-centimeter (0.362-in.) diameter. The ends were milled to length of 1.917 centimeter (0.755 in.). The pellets were cleaned ultrasonically, rinsed in methanol, and air dried, and were then fired in dry hydrogen at 1400° C for 6 hours. The pellets were stored in a vacuum desicator.

The pellet selected for use in the emitter specimen was vacuum ($<10^{-5}$ torr) fired at 1800° C for 30 minutes to remove gaseous and high-vapor-pressure impurities. The fuel was analyzed chemically and metallographically after the vacuum firing step. The results of these analyses are given in table I. The only significant contaminants were

nickel and silicon at levels of 65 and 90 ppm, respectively. These amounts are over the specification by 5 and 30 ppm, which is within the accuracy limits of the emission spectrographic analysis. The microstructure of the UO_2 fuel after the vacuum firing is shown in figure 2. The structure was essentially free of ceramic and metallic phases and was acceptable under the established fuel specifications.

Chemically vapor-deposited tungsten specimen cladding. - Material used in the cladding sleeve was produced by vapor deposition of WF_6 on a mandrel. Chemical analysis of this CVD W tubing is presented in table II. All impurities were within specification, and the material was chemically acceptable. To determine thermal stability, specimens of the as-received tubing were heat treated in vacuum at 2000° and 2500° C and then examined metallographically for grain size, second phase, and other microstructural irregularities. The as-received microstructure of the CVD W tubing is shown in figure 3 and appeared normal, with evidence of second-phase impurities. The grain size was measured as ASTM 6.6 to 6.8, and the microhardness was 522 to 528 Knoap's hardness number (KHN). The microstructure after the 2500° C heat treatment is also shown in figure 3. Swelling was not in excess of that specified, and the material was accepted for fuel cladding. The fabricated dimensions of the cladding sleeve (211A7568) were 1.181-centimeter (0.465-in.) in outside diameter, 0.965-centimeter (0.380-in.) in inside diameter, and 2.590 centimeters (1.020 in.) in overall length. The inside length between end caps was 2.006 centimeters (0.790 in.). Before assembly, all tungsten components were fired in wet hydrogen at 1000° C for 15 minutes and in vacuum (1.33×10^{-3} N/m^2 or 10^{-5} torr) at 1900° C for 20 minutes.

Arc-cast tungsten end caps. - Material used in the fabrication of the emitter end caps was vacuum arc cast tungsten rod, 1.905 centimeters (0.75 in.) in diameter. Chemical analysis results obtained for the vendor and a check analysis performed by the General Electric Company are compared in table III.

The hardness of the tungsten was specified to be 500 diamond pyramid hardness (DPH) under a 1.96-newton (200-g) load. The measured hardness was less than 470 DPH. A grain size of ASTM 6 or finer was specified, and the measured grain size was ASTM 8.0 or better. The microstructure appeared free of second phase, inclusions, or other defects considered detrimental to the intended application. The stem end cap (175A9832) was fabricated to a thickness of 0.254 centimeter (0.100-in.), and the bottom end cap (211A7536) to a thickness of 0.101 centimeter (0.040 in.).

Chemically vapor deposited tungsten central vent. - The material used for the central vent tube of the emitter specimen was produced as tubing by vapor deposition of tungsten fluoride (WF_6) on a steel mandrel. The purchased tubine had a 0.1777-centimeter (0.070-in.) outside diameter and a 0.0254-centimeter (0.010-in.) inside diameter. Chemical analysis results from the vendor are presented in table IV. The high iron (170 ppm) content and the trace of nickel was attributed to residue from the

steel mandrel used in the CVD process. To determine thermal stability, specimens of the CVD W were heat treated for 2 hours in vacuum at 2000° C for grain growth and at 2500° C for 1 hour for swelling. The microstructures after each treatment are shown in figure 4. The structure appeared to be clean and normal, and no cracks or voids were observed. The microhardness was measured as 541 KHN as-received and 496 KHN after the swelling test (2500° C). The measured grain size was 7.6 ASTM as-received and 6.7 ASTM after the 2500° C treatment. These values were within the GE specification of 550 KHN hardness and 6 to 8 ASTM grain size. The vent tube (211A7535) was machined to a 0.1270-centimeter (0.050-in.) outside diameter, a 0.0254-centimeter (0.010-in.) inside diameter, and a 1.295-centimeter (0.510-in.) overall length. Final heat treatment was at 1900° C in vacuum for 20 minutes.

Chemically vapor deposited tungsten - 22-weight-percent rhenium tubing for thermocouple stem. - The material used for the thermocouple stem (brazed to the top cap of the emitter) was produced as tubing by the codeposition of WF_6 and rhenium fluoride (ReF_6) on a mandrel. The CVD W-22Re alloy was used because of the need for ductility in this component. Chemical analysis results from the vendor compared with those performed by an independent laboratory are given in table V. All elements analyzed were within levels required by the specifications for chemical purity.

Maximum hardness specified was 475 DPH under a 0.0098-newton (100-g) load. The hardness of homogeneous material was measured as 470 DPH as-received and 410 DPH after 2500° C swell test. Metallographic examination of the as-received tubing revealed inhomogeneity in the form of a layered microstructure resulting from incomplete mixing of the WF_6 and ReF_6 gases before deposition. The microstructure is shown in figure 5. After the homogenization heat treatment at 2000° C for 2 hours, the material was not completely homogeneous, since layers were still present as shown in figure 5. After the 2500° C swelling test, the structure was homogeneous and free of sigma phase. This structure had a grain size of ASTM 7.4 to 7.7 and a microhardness of 410 DPH. The stem tube was treated at 2500° C for 1 hour for complete homogenization. The fabricated stem tube (175A8674) was 0.355-centimeter (0.140-in.) in outside diameter, 0.211-centimeter (0.083-in.) in inside diameter, and 1.461 centimeters (0.575-in.) long.

Niobium target disk. - The material used for the target disk (211A7537) was niobium sheet (0.0254 cm (0.010 in.) thick). This was double arc-cast material of 99.90 percent purity. The disk was fabricated to a 1.093-centimeter (0.43 in.) diameter with a 0.0254-centimeter (0.010-in.) diameter vent hole, 0.203 centimeter (0.080-in.) from the edge. The finished part was fired in vacuum (1.33×10^{-3} N/m^2 (10^{-5} torr)) at 1400° C for 15 minutes and stored in a vacuum dessicator prior to assembly.

Capsule fill gas atmosphere. - Analyses were performed by Stanford Research Institute (SRI) of gas from two sample cylinders charged in the glove box at the time the specimen capsule assembly was performed. The results are given in table VI. These analyses indicated a higher nitrogen and oxygen content than was specified. These results did not correlate with the research gas analyzer (RGA) and gas chromatographic analyses or with the clean welds obtained in the atmosphere box. The RGA analysis gave 64.4 percent argon and 34.1 percent helium. Gas chromatograph analysis at GE gave results of 2 ppm nitrogen and 2 ppm oxygen; no other impurities were detected. However, subsequent findings in the postirradiation examination and the fission gas analysis tend to confirm that the SRI analysis (see table VI) is typical of the atmosphere in the capsule assembly.

IRRADIATION TESTING

After fabrication and inspection by General Electric - NTPO, the capsule was shipped to the reactor site for irradiation testing.

Experiment 66-03-2 was first radiographed (fig. 6) and then installed in the reactor reflector position RB-2. Insertion by the vertical adjustable facility tube (VAFT) to reach the desired temperature levels was made during October 1969. The temperature differences between the two capsules were immediately so great that trouble was suspected, and the experiment was retracted. A radiograph (fig. 7) taken during the next cycle showed that a small amount of water had leaked into the 0.076 centimeter (30 mil) clad capsule. The experiment assembly was removed to the hot laboratory, where the defective capsule was cut away and replaced with an aluminum dummy. The leak later proved to be in the nickel-manganese (Ni-Mn) braze at the thermocouple penetration in the specimen and closure assembly and early failure of the remaining specimen capsule was anticipated. Since all objectives required a long running time, thermal cycling tests were substituted in hope that they could be completed before any failure occurred.

The experiment was reinserted in the reactor in January 1970. The maximum clad temperature was reduced to 1590° C for 190 hours, which allowed for redistribution. The radiograph (fig. 8) taken after this period showed complete redistribution.

Fifty short thermal cycles were made during March 1970. A typical temperature-time plot of these cycles is shown in figure 9. Radiography showed the capsule structure and fuel condition to be unchanged. To get a lower minimum temperature, the experiment was moved to a new reflector position, where 24 long thermal cycles were made during June 1970. The typical temperature-time profile for the long cycle is shown in figure 10. The radiograph (fig. 11) taken after the series of cycles showed the bottom end cap to be bowed downward approximately 0.0127 centimeter (5 mils). No other changes were apparent.

A bent capsule instrumentation lead tube was discovered during reinstallation, and removal to the hot lab was necessary for repair. The capsule was returned to the reactor in July 1970 to continue life testing. Radiographs (fig. 12) taken at 634 hours showed that the high-temperature thermocouple stem had broken and the specimen had shifted downward slightly. The likelihood of future shifting made controlling by means of temperature unreliable. However, the ΔT between the outer can thermocouple and the cooling water had been considered a good indication of power generation before the stem was broken. Investigation of the probable heat paths after the break and again after the subsequent bottoming of the specimen indicated that the heat balance had changed only a small amount. Therefore, it was assumed that maintaining the ΔT at prebreak levels would keep the temperatures in the specimen approximately the same as before.

The remainder of the test was run at constant power using the output of the self-powered neutron detectors and the outer can thermocouple as a control input.

The next radiograph was taken at 1554 hours (fig. 13) and showed that the specimen had now slipped to the bottom of the capsule and the bottom end cap had continued to bow downward. There was still no obvious diametral swelling. The life test was terminated with the radiograph taken at 2607 hours (fig. 14) which revealed bottom end cap failure.

Table VII gives a chronological accounting of some test parameters with remarks and also indicates when neutron radiographs were taken.

POSTIRRADIATION EXAMINATION

Scope of Examination

The postirradiation disassembly and examination of the capsule from experiment 66-03-2 was performed in the GE Evendale Radioactive Materials Laboratory (RML). The scope of this hot-cell examination includes:

(1) Visual examination of the capsule and components
(2) Removal and analysis of the flux wires
(3) Gamma scanning of the capsule and fuel specimen
(4) Puncturing the capsule and analysis of the fission gas
(5) Disassembly of capsule and inspection of fuel specimen
(6) Examination of fuel specimen, dimensional measurements, and gamma scan
(7) Removal of bottom catcher plate and analysis of deposit
(8) Test for communication between fuel cavity and vent tube outlet
(9) Sectioning of fuel specimen for metallography and fuel analysis
(10) Complete metallographic examination of longitudinal and transverse sections and central vent tube

(11) Analysis of bottom cap weld failure

(12) Gamma autoradiograph of fuel sections to show burnup gradient

(13) Radiochemical analysis for fuel burnup.

Capsule Disassembly Operation

After making final neutron radiographs in PBR, the capsule was cut from the insertion rod in the Plum Brook Hot-Cell Facility and loaded into an approved shipping cask for transporting to GE-NSP in Evendale, Ohio. The irradiated capsule was delivered to the GE-NSP Hot Cells on March 19, 1971.

Visual examination. - The condition of the capsule on arrival at the hot cell is shown in figure 15. The surface appeared dull and mottled from exposure to reactor water. No blemishes or damage from handling was observed. The outer shroud was removed by drilling out the rivets at the top and pulling out the capsule holder and components (see fig. 16). The holder contained the capsule number 2 and the dummy insert, which replaced capsule number 1 early in the experiment.

Throughout the disassembly operations care was exercised to maintain the orientation of the containment can and the fuel specimen with respect to the side facing the reactor core or peak flux during irradiation. During assembly of the 66-03-2 capsule certain index marks were used to maintain orientation and instructions were given for insertion of the capsule in the PBR with respect to the reactor core. Assuming that those instructions were properly carried out at the test site, the marking "N" on the frame of the capsule (fig. 16) and correspondingly the pinched-off gas fill tube at the top of the steel container (fig. 17) would have faced peak flux during irradiation.

This orientation was carried over to the clad fuel specimen when the container was cut open, but, since the stem tube had broken during test, it was necessary to match the broken ends together to establish orientation with the steel container. This match was confirmed by an index mark on the top end cap of the fuel specimen. Further confirmation that the proper orientation had been maintained and identified during disassembly was obtained from subsequent fuel burnup analyses showing higher burnup on the side facing the reactor core and also from gamma autoradiographs of fuel sections showing greater fuel thickness on the side identified as facing peak flux.

The steel capsule containing fuel specimen number 2 was removed from the holder with the thermocouple leads intact. The capsule was photographed at four orientations as shown in figure 17. There was no noticeable difference in appearance of the side facing peak flux and the side away from peak flux (south). The surface appeared mottled at each end of the capsule while the midsection was bright, indicating a higher operating temperature in the area of the fuel specimen.

The nickel-manganese braze alloy around the thermocouples at the top of the capsule showed evidence of corrosion by the reactor water, but it had not deteriorated enough to allow a leak into the capsule. This brazed area is shown in figure 18.

Flux wire analysis for thermal and fast flux. - Flux wires were contained in two aluminum tubes, one on each side of the specimen holder at 90° to the fuel specimens. These flux wire tubes were removed during the capsule assembly and shipped to the GE Vallecitos Laboratory for analysis. One of the two wires of each pair was made of an aluminum-cobalt alloy containing 93.3 ppm cobalt, and the other was type 304 stainless steel. These wires were counted for cobalt-60 and manganese-54. Only the long-lived fission products or neutron activation products were present in sufficient quantity to affect the gamma profile. The fuel redistribution at either end of the fuel pellet was indicated by prominent concentrations of gamma activity in these locations. The traverse over the fuel pellet indicated a somewhat greater concentration of activity in the fuel near the bottom end cap and around the vent tube, with a gradual decrease as the scan approached the top end cap. This indicated nonuniform fuel burnup or nonuniform fuel redistribution over the length of the specimen. Examination of the neutron radiograph indicated that nonuniform fuel redistribution contributed most to the observed gamma scan profile. The peak width on the scan in areas outside the fuel specimen indicated relative width of the gamma producing sources. Peaks 1 to 3 were relatively narrow corresponding to narrow gamma emitting sections. Peaks 7 and 8 showed less definition, which is indicative of commonality caused by braze material concentration separated by thin braze segments. The total peak width indicates a braze band of 0.28 centimeter (0.11 in.), which compares favorably with the neutron radiograph. The energy resolution of the identified gross gamma peaks was performed using the 400-channel analysis in the pulse-height analysis mode coupled to a 5-centimeter (2-in.) sodium iodide internal line detector. Standards used for peak location were mounted sources of cobalt-60 and cesium-137. The iron concentration in the stainless-steel samples was determined spectrophotometrically followed by ion-exchange separation of the manganese-54 before counting.

To relate the raw counts to fluence, it was assumed that the flux spectrum of the PBR was similar to that of the G.E. fast reactor. The same assumption was made for the analysis of the previous experiment, PBR 66-03-1 (ref. 3). The values of the cross section used were 42.3 barns for the $^{59}Co\ (n, \gamma)\ ^{60}Co$ reaction and 0.086 barn for the $^{54}Fe\ (n, p)\ ^{54}Mn$ reaction. A Watts fission spectrum was used above 1 MeV. The accuracy of these results is estimated to be ±50 percent. Table VIII shows the results.

Capsule gamma scan for peak activity. - Using a 400-channel analyzer with a motor drive fixture in the hot cell, a gross gamma scan was performed over the length of the containment can using a Cobalt-60 standard. The activity was recorded with an x-y plotter. A plot of the gross gamma scan is shown in figure 19 with a corresponding

neutron radiograph of the capsule for a direct comparison of capsule components, including the fuel specimen, and the activity associated with them.

The gross gamma traverse of the containment can length indicated eight significant peaks of gamma activity occurring in the bottom of the stainless-steel containment can, at the niobium heat shields and niobium catcher plate, at each end and at the midplane of the fuel pellet, at the Palco braze joint, and on the stainless-steel thermocouple stem. Because of the 4-month interval between irradiation and gamma scanning, pulse-height analysis of the energies within the individual peaks indicate that the activity was predominantly from fission products, with a contribution of cobalt-60 at several locations. Zirconium-95 - niobium-95 was predominant in the fuel pellet area and was absent from all other areas, except for a small amount at peak 3. Cesium-137 predominated at several points and may have been present in the fuel region but was obscured by the magnitude of the zirconium-95 - niobium-95 peak. Energy resolution of the activity comprising the individual peaks is described next.

Peak 1 displayed activity that was predominately cesium-137, which is indicative of the plate-out concentration of this fission product in the bottom of the containment can.

Peak 2 displayed cesium-137 (and a trace quantity of ^{60}Co) at the niobium heat shields.

Peak 3 was composed of cesium-137 with contributions of zirconium-95 - niobium-95 and trace quantities of cobalt-60 at the catcher plate or bottom end cap.

Peaks 4 to 6 displayed identical energy distributions in the fuel pellet. The predominant activity was zirconium-95 - niobium-95. Cesium-137 may have been present and obscured by the magnitude of the zirconium-95 - niobium-95 peak.

Peaks 7 and 8 displayed the presence of only cesium-137 and cobalt-60. The cobalt-60 peak was contributed by the lead-cobalt braze used to join the stem to the steel container.

The general distribution of cesium-137 was indicative of the loss of volatile fission products from the fuel pellet after the rupture of the bottom end cap weld with subsequent distribution of cesium-137 throughout the steel containment can. The detection of cobalt-60 in trace amounts at several peaks would be expected since the containment can components were fabricated of austenitic stainless steel.

Container puncturing and fission gas analysis. - As part of the post-test analysis, the stainless-steel containment can was punctured; the gases were collected in a stainless-steel bottle and analyzed for constituents by gas chromatography and gamma counting. The results of these analyses were compared with calculated fission gas production to assess the degree of fission gas release from the fuel. In addition, calculations were made of the fission-gas production at the end of the irradiation.

The apparatus for puncturing the container and collecting gas for analysis was pumped down to 1.0×10^{-2} newton per square meter (10^{-4} torr), heated and outgassed for

4 days with a dummy capsule in the drilling fixture and with the charcoal-filled collection bottle attached. The drilling procedure was practiced using remote manipulators in the hot cell to drill through the vacuum seal into the dummy capsule. With the bottle closed off, the irradiated container was placed in the drilling fixture, and the apparatus was pumped down to 2.0×10^{-2} newton per square meter (1.5×10^{-4} torr) and held at this pressure for several hours. The leak rate was measured at less than 1 micrometer per minute. With the pump valves shut off the container was punctured by drilling through the side wall at a point above the top of the emitter specimen. Successful puncturing was indicated by an immediate off-scale reading of the ion gage. The fission gas sample was collected in the charcoal-filled steel bottle, which was immediately submerged in liquid nitrogen to condense the gas in the bottle. After 2 hours, valve to the gas sample bottle was shut off with a negative pressure of 29 to 30 inches showing on the gage (9.83×10^{4} to 10.15×10^{4} N/m^2). The bottle with valve and gage attached was removed from the system, and a pipe sap was attached to insure a positive seal for transporting the bottle.

The bottle was shipped to the GE Vallecitos Laboratory for analysis. Two analyses were performed: one of a gas sample taken from the gas bottle at room temperature, and the second sample taken after the bottle was heated to 360^{o} C. The second sample was taken to drive off gases, especially xenon, adsorbed on the charcoal in the sample bottle. The second analysis gave more reasonable values for the xenon concentration but also gave a high percentage of carbon dioxide (641 percent, 6.314 cm^3), probably from the heated charcoal. Table IX(a) shows the measured results, the absolute volume of each constituent, for the second analysis only.

The absolute volume of each constituent was computed by taking the volume of the bottle and the chromatograph manifold, the system temperature and pressure, and then reducing the volume to standard conditions. The volume is then simply the product of the measured fraction of each constituent times the total volume at standard conditions. Since the manifold volume was only 12 cubic centimeters compared with nearly 500 cubic centimeters for the bottle, the error introduced by taking a second sample was quite small, about 2 percent, which is less than the reported accuracy for the analysis itself.

Table IX(b) shows the volume percent comparison of only argon, helium, and nitrogen with the SRI analysis of the gas injected during capsule fabrication. Postirradiation volume percent shown on table IX(b) were taken from the second gas analysis. The discrepancy between the preirradiation and post irradiation results is believed attributable to the loss of helium by diffusion from the sample bottle over the long time period between puncturing the capsule and analyzing the sample.

The production of the fission gases, xenon and krypton, was calculated using a time share version of the GE-NSP CHAINS code (ref. 5). This code follows the production and decay of radioisotopes using an arbitrary exposure history. Nuclear data were

taken from the published literature (refs. 6 and 7). In practice, only two chains of isotopes had to be computed, krypton-85 and xenon-136 (from ^{135}Xe). The measured number of fissions was used, as will be discussed in the section Burnup analysis of fuel.

The following scheme was used to calculate the xenon-136 produced from neutron capture in xenon-135:

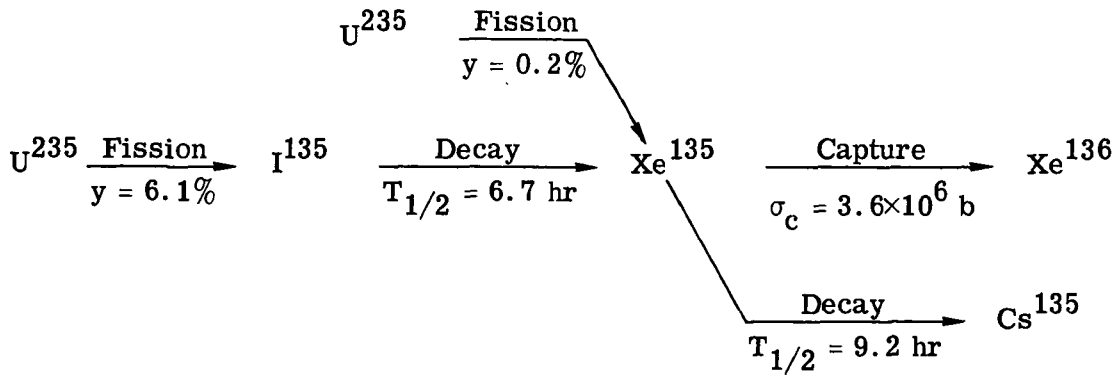

Table IX(c) shows that the total krypton and krypton-85 measured values are about 63 percent of that calculated from the fuel burnup. The measured xenon is about 43 percent of that calculated. A lower amount of fission products than that calculated from the burnup analysis was expected because some of these products were still trapped in the UO_2 fuel. But these values were much lower than expected, the reason for which is discussed in the section Deposition of Fission Products.

Table X shows the various isotopes of interest and their yields. The calculated end-of-irradiation yields from table X give 0.232 cubic centimeters at standard temperature and pressure for krypton and 1.569 cubic centimeters for xenon, for a total of 1.822 cubic centimeters at standard temperature and pressure. No attempt was made to calculate the yields of other fission products that may be gaseous at operating temperature, since this depends, in part, on the chemical combinations and temperature gradients.

Fuel Specimen Examination

Disassembly of container. - Using a thin silicon carbide cut-off wheel, the steel containment can was cut transversely in the area of the broken stem, as determined from the neutron radiographs. The fuel specimen was easily removed from the container. The surface of the tungsten cladding appeared clean and undamaged (fig. 20). The side of the fuel specimen that was oriented toward the reactor core (peak flux) during irradiation was identified. This orientation of the side toward peak flux was con-

firmed by an index mark on the top end cap (fig. 20) and was thus maintained throughout the subsequent metallographic examination of the fuel specimen.

Visual examination of cladding. - Examination of the cladding surface using periscope binoculars at magnifications up to ×50 revealed no defects in the tungsten cladding sleeve or any indications on the outside diameter of failure at the bottom end cap. In subsequent metallographic examination of a transverse section, a single crack was observed that penetrated the CVD W cladding wall, but no evidence of such a crack was observed during the clad surface examination. A foreign deposit, observed on the bottom of the fuel specimen, nearly covered the niobium catcher plate as shown in figure 21. This deposit was pried loose from the bottom of the specimen, and the deposit proved to be very friable. Subsequent analysis by X-ray fluorescence identified the deposit as niobium, and by X-ray diffraction analysis it was found to be a niobium-nitrogen-oxygen compound.

Re-examination of the interior of the stainless-steel container revealed that parts of the three niobium heat shields in the bottom of container were missing. As part of the subsequent metallographic examination, the bottom of the steel container was filled with epoxy and was sectioned longitudinally and polished to examine the remains of the heat shields and molybdenum retainer ring. This revealed that the molybdenum ring was intact but that the three niobium heat shields adhered to the bottom of the catcher plate. It was concluded that the niobium heat shields had reacted with impurities (N_2) in the helium-argon cover gas. When the thermocouple stem broke during irradiation and the specimen dropped down to the bottom of the containment can, the contaminated niobium heat shields apparently became bonded to the bottom catcher plate of the specimen.

Further examination of the interior of the upper half of the steel container revealed a dark crystalline deposit on the walls, with the heaviest deposit in the cooler areas as shown in figure 22. Chemical analysis of this deposit was not made.

Clad gamma scan. - Gamma scanning was performed over the length of the fuel specimen in the same manner as described previously for the container scan. Three peak activity areas were indicated corresponding to the same three peaks for the container over the fuel specimen. These were at each end of the fuel pellet, where major redistribution of fuel had occurred, and at the midsection of the fuel. The correspondence of these peaks for the specimen and the container indicated that no fuel or fission-product deposits were on the container walls around the specimen.

Dimensional evaluation of clad-fuel specimen. - Dimensional measurements were made of the fuel emitter specimen in both diameter and length and compared with the as-built dimensions. The measurements were made directly with micrometers using remote handling manipulators of the hot cell. Diametral measurements were made at 0° and 90°, where 0° was on the side facing peak flux in the reactor. Eight readings

were made from the top end cap to the bottom catcher plate, approximately 0.317 centimeter (1/8 in.) apart in each direction. Calibrated micrometers reading to 0.0002 centimeter (0.0001-in.) were used. Two sets of readings were taken in an effort to average out slight errors induced by the remote handling manipulators. The two sets of diametral measurements are given in table XII. The diametral growth in the cladding was plotted in relation to the fuel specimen length, as shown in figure 23.

The curves were drawn through the highest points of the two sets of measurements, rather than the average values, to show the maximum possible diametral swelling of the cladding at each point measured. The two readings at diameter C, in line with peak flux, were judged to have been read and/or recorded erroneously because the points are 0.005 centimeter (0.002 in.) less than adjacent readings. Furthermore, the tips of the micrometers were larger in diameter than the spacing between measurements, so that each measurement overlapped the adjacent measurement. The maximum growth measured was 0.015 centimeter (0.006 in.) on the peak flux diameter. The accuracy of these measurements was confirmed in subsequent metallographic examinations when the diameter of transverse sections at positions E and F (fig. 23) was measured microscopically and agreement withon 0.002 centimeter (0.001 in.) was obtained. These data are given in the section on metallographic examination.

Length measurements were made at four points around the ends of the cladding sleeve. Accurate measurements could not be made because the bottom retainer ring projected below the bottom of the shroud. The length ranged from 2.920 centimeter (1.149 in.) on the side toward peak flux to 2.930 centimeter (1.153 in.) at a line 90^{o} from the peak-flux measurement. The as-fabricated sleeve length before welding was 2.605 centimeter (1.025 in.). Length measurements were not made on the assembled emitter before irradiation, so it is not known how much was added to the overall length by the retainer ring and the top weld bead.

Catcher plate deposit analysis. - To avoid fracturing the tungsten cladding, the fuel specimen was encased in epoxy with the catcher plate exposed. No epoxy was permitted to get inside the fuel. The tack welds were then ground away from the retainer rings, and the rings were removed. The catcher plate could not be removed readily, so the fuel specimen was clamped under the cut-off wheel and, after a partial cut into the tungsten shroud, the catcher plate broke away with the shroud ring intact.

On the inner surface of the catcher plate opposite the central vent tube was a deposit of black crystalline material presumed to be UO_2 (fig. 24). Subsequent survey of the catcher plate indicated activity of 18 R at contact and 2 R at 15.2 centimeters (6 in.). The niobium catcher plate was completely dissolved in nitric/hydrofluoric acids (nitric acid alone did not remove all the uranium and fission products from the niobium) and aliquots were taken for uranium and fission product analyses. The uranium content was determined by spiking with a known amount of ^{233}U followed by mass spectrometric

measurements of the $^{233}U/^{238}U$ and $^{233}U/^{235}U$ ratios. The major fission products were determined by gamma-ray pulse-height analysis. Table XIII shows the results.

These results can be compared with the total amount originally present (in the case of uranium) or expected because of fissioning (in the case of cerium). For the two uranium isotopes, the amount on the catcher plate was 0.053 percent for ^{235}U and 0.059 percent for ^{238}U. By contrast, 0.08 percent of the calculated ^{144}Ce was measured on the catcher plate. This result may be due to the higher volatility of cerium with respect to uranium dioxide. Calculations of the production of the other isotopes was not attempted because of their relatively short half-lives when compared with the irradiation time.

These results confirm that a considerable quantity of UO_2 and fission products escaped either through the vent tube or through the rupture in the end plate weld.

It was predicted by Wilkins (ref. 8) that the fuel loss rates through the central vent would be 0.33 milligram per year with a fission gas pressure of 1.3 kilonewtons per square meter (10 torr) and 0.25 milligram per year with a gas pressure of 13 kilonewtons per square meter (100 torr). The fusion gas pressure of the steel containment can at the time of puncturing and sampling the fission gas was calculated to have been 4.65 kilonewtons per square meter (35 torr). Therefore, Wilkins' predictions for this pressure would have been about a 0.3-milligram-per-year fuel loss through the vent. The total irradiation time of 2607 hours for experiment 66-03-2 is equivalent to 0.3 year, and the predicted fuel loss would be only 0.09 milligram.

The analysis of the deposit on the catcher plate showed 0.855 milligram of ^{235}U and 4.93 milligram of ^{238}U. This is more than 60 times the predicted fuel loss through the central vent tube. However, this is not surprising in view of the weld failure at the bottom end-plate, which could have occurred early in the irradiation test (as early as 410 hours into testing when dishing of the bottom cap was first observed) and provided a free escape path for fuel and fission products. This end cap failure plus the fracture of the central vent tube during irradiation negated any valid comparison between Wilkins' predictions for fuel loss and actual measured amounts of fuel on the catcher plate.

End-cap weld rupture. - The two inner retainer rings between the catcher plate and the bottom end cap were then removed. This exposed the weldment joining the end cap to the tungsten sleeve. The end cap had broken away from the weld nearly halfway around the sleeve and the cap was pushed out toward the catcher plate, although it apparently had not touched the catcher plate. A black crystalline deposit on the end cap extended from the central vent tube to the area of the rupture in the weldment. This is shown in figure 25. Based on the orientation of the fuel specimen with respect to peak flux as established at disassembly of the capsule, it was apparent the major portion of the weld rupture was on the side away from peak flux. An analysis of the end-cap weld failure will be discussed as part of the metallographic examination.

Communication test for gas transport through vent. - For the central vent tube to be effective in removal of fission gases from the fuel, the tube must remain open. A simple test was made, checking for communication of gases from the fuel cavity to the vent-tube outlet. A carbide-tipped drill (0.203 cm (0.080 in.)) was used to penetrate the central cavity through the 0.102-centimeter (0.040-in.) thick CVD W clad wall and the fuel core.

This hole was drilled on the side that faced peak flux and in the upper half of the specimen where a subsequent transverse cut was to be made for metallographic study. To demonstrate that communication existed, a tapered Teflon tube was fitted into the drilled hole, and the specimen was submerged in methanol. Air was easily forced through the vent exit as evidenced by the evolution of bubbles in the methanol. With only slightly higher pressure, bubbles also evolved from the ruptured area around the bottom cap. It was concluded that for room-temperature conditions the vent tube was open between the fuel cavity and the cover gas volume.

Sectioning of fuel emitter specimen. - The fuel specimen was impregnated with clear epoxy by submerging the specimen in liquid epoxy and curing it in a vacuum oven. This was done to insure that all components remained in place during fuel sectioning. Two transverse cuts were made (fig. 26), one through the upper half where the hole had been drilled through the side and a second cut near the midpoint of the specimen but above the tip of the vent tube as determined by neutron radiographs. In this manner a thin section through the fuel was obtained for fuel burnup analysis.

The two transverse sections were polished, and measurements of the diameters of the transverse sections were made using the microscopic crosshairs as index and measuring the table travel with a dial gage. These accurate measurements confirmed the diametral measurements made in the hot cell with micrometers, as shown by the following table:

	Microscopic measurement		Micrometer measurement	
	cm	in.	cm	in.
Section F:				
Diameter 0° to peak flux	1.1953	0.4706	1.1973	0.4714
Diameter 90° to peak flux	1.1955	.4707	1.1933	.4698
Section E:				
Diameter 0° to peak flux	1.1964	.4710	1.1945	.4703
Diameter 90° to peak flux	1.1897	.4684	1.1903	.4687

After metallographic examination of the transverse sections had been completed, the upper part of the fuel specimen was sectioned longitudinally on the axis through the thermocouple stem tube, and both longitudinal faces were polished for metallographic examination (sections 104 and 105 of fig. 26). Longitudinal sectioning of the lower half of the specimen presented a problem because the vent tube appeared to be at an angle to the axis and it was desired that it be sectioned in a plain parallel to the vent tube, as well as through the failed weldment at the bottom cap. Therefore, the section was remounted in epoxy with the visible end of the vent tube at the bottom of the mounting. A longitudinal section was then cut off-center and parallel to the vent tube. This resulted in a section through the endplate at the defect area for metallographic examination.

Metallographic examination of clad fuel specimen. - Upper section: The transverse section 1 (fig. 26) of the upper part of the clad fuel specimen was cut approximately 0.76 centimeter (0.3 in.) from the top of the specimen end cap. This transverse section was polished, and the microstructure was examined for evidence of chemical reaction between the UO_2 fuel and the CVD W cladding. At the interface between fuel and cladding shown in figure 27, no evidence of gross interaction was observed, based on no grain-boundary precipitates or intergranular penetration of the cladding. The fuel temperature in this region during irradiation was estimated to be 1700° C.

The typical microstructure of the CVD W cladding in this upper transverse section is shown in figure 28. Except for grain growth, the columnar structure appears little different from the pretest condition shown in figure 3.

The transverse mounting of the upper portion of the clad fuel emitter was then sectioned longitudinally through the center of the stem tube. The half-sections were remounted and polished. Section 105 was used for metallographic analysis and photomicrographs.

The top end cap and the tungsten-rhenium stem tube were joined with molybdenum-rhenium braze alloy. As shown in figure 29, the braze was sound and showed excellent stability with the two components. This area during irradiation was at a temperature of 1500° C or higher.

Intergranular cracks developed in the arc-cast tungsten end-cap beneath the thermocouple well (fig. 30). This cracking was attributed to thermal-mechanical stresses developed in the thin (0.076 cm (0.030 in.)) section under the thermocouple well as a result of brazing of the tungsten-rhenium stem tube. This cracking would have lead to early failure of the top end cap with continued irradiation. The joint of the arc-cast tungsten top end cap to the CVD W cladding sleeve was made by electron-beam welding on the top face. In addition, three spike welds were made about 0.038 centimeter (0.015-in.) apart around the cladding sleeve with full penetration to the end cap. A longitudinal section of this welded joint (fig. 31) reveals a crack in the CVD W cladding at the point of the lower spike weld. This type of cracking would have lead to early

failure of the cladding with continued irradiation.

The microstructure of the redistributed UO_2 fuel under the top end cap of the fuel specimen is shown in figure 32. A fine metallic phase was scattered through the redistributed fuel. This phase was not identified, but it is assumed to be metallic fission products or some other metallic impurities present in the UO_2 before irradiation. The large cracks in the fuel resulted from thermal shock and shrinkage on cooldown.

Lower section: In the initial sectioning of the fuel specimen two transverse cuts were made near the midpoint of the specimen as previously described (fig. 26). The cross section of the lower half of the fuel specimen (No. 102) was taken at a plane approximately 1.42 centimeter (0.56 in.) from the bottom end of the fuel specimen. This was calculated to cut through the fuel just above the tip of the central vent tube, based on the location shown in the final neutron radiograph. It was found later that the central vent tube had fractured at the bottom end cap joint and had broken loose during posttest handling. This condition was not known at the time of epoxy impregnation and subsequent sectioning; it is possible that the cut was made through the upper end of the vent tube. However, the end of the tube did not appear in the cross-sectional cut, and grinding down was required until the tip of the tube was exposed.

At this point, it was noted that the end of the vent tube was lying against the wall of the fuel cavity. This condition was attributed to the bowing of the bottom end cap resulting in tilting of the vent tube. As will be discussed later, the tube had fractured, and part of it was lying against the wall of the fuel cavity.

The microstructure of the CVD W cladding at the midsection of the fuel specimen is shown in figure 33(a). When compared with the pretest microstructure (fig. 3), considerable grain growth and change in grain geometry was observed. However, no gross interaction with the UO_2 fuel or grain-boundary separation was observed like that of previous experiments (ref. 3). A single crack through the wall was found in this transverse section as shown in figure 33(b). This was an intergranular type of cracking and is attributed to deformation of the cladding imposed by mechanical swelling of the fuel during irradiation. Similar localized cracking in the grain boundaries of the CVD W cladding was also observed in the longitudinal section as shown in figure 34.

Examination of the fuel-cladding interface in both transverse and longitudinal sections revealed no evidence of any gross interaction between UO_2 fuel and the CVD W cladding, (figs. 34 to 37). Although fine porosity (gas bubbles) was observed in the grain boundaries of the tungsten cladding, no evidence of any grain boundary constituent or second phase was observed in these metallographic sections. The tungsten clad thickness measured 0.1041 centimeter (0.041 in.), which indicates no change during irradiation.

The microstructures of the UO_2 fuel at the midsection of the fuel specimen are shown in both transverse and longitudinal sections in figures 36 and 37. These struc-

tures are typical of completely redistributed UO_2. Columnar grains formed from outside to center by the migration of lenticular pores to the center. The temperature gradient across these fuel sections have been calculated to be approximately 560° C. This is reflected by the grain structure and void formation. At the fuel-cladding interface is a layer of porous UO_2 formed by vapor condensation on the cooler wall of the cladding. The large voids that formed between the columnar grains decrease in size and quantity near the central cavity where fuel isotherm temperature was calculated to be 2250° C during irradiation. The very small spherical voids are assumed to be fission gas bubbles collecting in the grain boundaries. Small spherical metallic particles observed in the UO_2 near the central cavity as shown in figure 37 are assumed to be metallic fission products, impurities in the UO_2, or tungsten. Large radial and circumferential cracks observed in the fuel pellet are attributed to thermal cycling during inpile operation.

Measurements of the transverse section of fuel at the midsection of the specimen indicated that redistribution had reduced the fuel pellet wall thickness by 0.064 to 0.096 centimeter (0.02 to 0.038 in.).

Vent tube fracture. - As discussed previously, when the bottom half of the fuel emitter was ground on the transverse cross section until the tip of the vent tube was exposed, the vent tube was on one side of the fuel cavity, and the end of the tube was cracked with large grains of the CVD W missing as shown in figure 38 and 39. No fuel deposits were observed on either inside or outside diameter surfaces of the vent tube in this transverse section. There was also no evidence of any gross interaction between the CVD W tube and the fuel. A comparison of the grain growth in the CVD W vent tube shown in figure 39 with the grain size of the original CVD W tube after the 2500° C swelling test shown in figure 4 indicates that the tip of the vent tube operated at temperatures greater than 2200° C.

After complete metallographic examination of the transverse section of the lower half, it was remounted in epoxy. It was assumed that the vent tube was still attached to the bottom end cap and was tipped at an angle to the axis of the specimen. Therefore, cutting longitudinally in a plain parallel to the vent tube as well as the axis of the specimen gave a section that could be ground by increments into the vent tube and also into the ruptured weld at the bottom end cap.

Incremental grinding of the longitudinal section continued until the wall of the vent tube was exposed; the mounting was then polished and examined. As shown in figure 40, the vent tube had broken away from the bottom end cap and was lying in the fuel cavity parallel to the axis of the specimen. Measurements of the length of this piece of vent tube indicated less than half of the as-fabricated length of 1.19 centimeter (0.47 in.) remained. Since the upper end of the vent tube was broken in the transverse section and fractured in the longitudinal section, it was concluded that the upper end of the vent

tube was cracked during posttest handling and shipping when the tube was free to tumble in the fuel cavity. Neutron radiographs of the capsule after the last irradiation cycle show that the vent tube was on center in the fuel cavity but that the tip of the tube was raised approximately 0.127 centimeter (0.050 in.) higher than the pretest position.

Incremental grinding was continued into the wall of the vent tube until the central hole was exposed and the surface of the inside diameter could be examined. No evidence of fuel deposits were found in the bore of the vent tube. The polished section of the vent tube after grinding into the inside diameter is shown in figure 41. The enlarged hole at the lower end resulted from a 0.050-centimeter (0.020-in.) diameter counterbore made to depth of 0.25 centimeter (0.10 in.). Also shown are scattered deposits of UO_2 at the walls of the enlarged hole.

A small deposit of UO_2 was also found on the outside of the vent tube near the fractured base as shown in figure 42. This is believed to have been part of the miniscus of redistributed fuel at the base of the vent tube as shown in the neutron radiographs prior to fracture of the tube.

During the incremental grinding of the vent tube, the bottom end cap and adjacent fuel were also examined at several levels. These polished sections revealed that the central vent tube had fractured and broken off at the inside weld adjacent to the bottom end cap (fig. 43). Furthermore, the cavity in the fuel pellet where the vent tube had been before fracturing occurred was filled in with redistributed fuel (figs. 43 and 44). Measurements of the thickness of this fuel deposit in the tube cavity showed about 0.101 centimeter (0.040-in.) thickness. This suggests that the vent tube was fractured before the last cycle of irradiation, but remained in position during the neutron radiography and reinsertion into the reactor. However, the tube remained approximately upright as viewed in the neutron radiograph (note, fig. 4) since the tube end was held in the socket formed by the fuel cavity, as shown in figure 43. During subsequent handling and shipping of the capsule, the vent tube probably fell into the upper part of the fuel cavity, and the tip was broken as the tube tumbled in the cavity. The redistributed UO_2, which bridged the cavity left by the fractured vent tube, contained a large amount of metallic second phase as shown in figure 44. This second-phase material was deposited in horizontal layers, which suggests that it may have resulted from solutioning of the CVD W tube in the UO_2.

Analytical samples of this redistributed fuel were obtained by drilling with a diamond core drill into the polished section. The first sample consisted of fine powder drillings, and the second sample consisted of coarse particles that broke out of the microstructure during drilling, since the fuel deposit containing the second-phase material proved to be a thin bridge across the gap (fig. 44).

These two fuel samples were initially analyzed by X-ray diffraction techniques, but the X-ray scans were negative because of the high gamma activity of the fuel samples.

Efforts to shield the film in the powder camera using nickel foil proved ineffective. The samples were then ground to fine powder and combined for analysis by X-ray fluorescence. This technique was successful in detecting the elements uranium, tungsten, iron, and nickel. The relative amounts of these elements or the form in which they were present could not be determined from this very small powder sample.

The source of iron and nickel can be traced to both the UO_2 fuel pellet, which was analyzed and found to contain 25 ppm iron and 65 ppm nickel (table I), and to the CVD W vent tube, which contained 170 ppm iron. During irradiation, the fuel temperatures in this area may have exceeded the melting points of these (Fe and Ni), causing them to alloy with tungsten or uranium. The microstructure of the metallic phase in the redistributed fuel of figure 44 has the appearance of having been in the molten state during irradiation. These findings suggest that the broken end of the central vent tube may have been solutioned by the lower melting elements and precipitated in layers as shown in figure 44.

Bottom weld joint rupture. - In previous discussions of the visual examination of the fuel specimen, it was noted that the bottom end cap was pushed out on the side away from peak flux and that the weld joint had ruptured nearly halfway around the cladding sleeve (see fig. 25). The longitudinal sections of the lower half of the fuel specimen were cut so that one side contained the apparent sound weld joint and the other side (containing the vent tube) could be ground into the area of the ruptured weld.

Examination of the weld joint on the unruptured side revealed that cracking had initiated at the inside corner of the joint and proceeded down the center of the weld zone nearly to the outside edge as shown in figure 45. Grinding further into this sound weld area and polishing revealed the structure shown in figure 46 where the crack in the weld was just starting. This shows that full penetration was achieved by the electron-beam welding of the 0.101-centimeter (0.040-in.) thick arc-cast tungsten end cap to the CVD W cladding sleeve but that the affected zone was very narrow, as shown by the unaltered grain size of the CVD W cladding adjacent to the welded joint.

The microstructure of the ruptured weld joint in the opposite side of the specimen is shown in figure 47. Considerable bowing and distortion of the arc-cast tungsten bottom end cap is evident. This caused sufficient stress on the weld joint to produce intergranular cracking and rupture of the bottom weld. A similar condition existed (but not as pronounced) in the electron-beam weld at top end cap as noted previously (fig. 31).

In all sections examined, the cracking appeared to have proceeded along the original interface between the two components and at the boundary between two very different microstructures. This suggests that a larger weld bead at such joints would be desirable to achieve a wider zone of uniform microstructure. However, allowances for shrinkage in the electron-beam weld must be considered to avoid stresses on the cladding components. In this case, a redesign of the weld joint would be recommended to avoid stresses due to shrinkage in the weld.

Gamma autoradiographs of fuel sections. - Gamma autoradiographs were made by placing the polished sections of the fuel specimen face down on high-resolution glass photographic plates in contact with the emulsion and giving each an exposure of 30 seconds. Enlarged prints of the transverse sections (fig. 48) shows less fuel thickness on the side toward peak flux and a minor gradient in the fuel burnup from outside to center. The hole was drilled on what was considered to be on the peak flux side. These autoradiographs (fig. 48) confirm reasonably well the orientation that had been established earlier in the examination. Several large radial cracks were evident in the bottom section of the fuel pellet, and the broken vent tube was apparent on one side of the cavity. In the longitudinal sections of the fuel pellet (fig. 49), the top section shows lower fuel burnup at the center, which was immediately below the thermocouple well in the top end cap; the bottom section shows several large radial cracks, redistributed fuel, and a piece of the broken vent tube in the cavity and at the central vent hole. Bowing of the bottom end cap by swollen fuel is clearly shown in the autoradiograph.

Burnup analysis of fuel. - During the sectioning of the fuel specimen, a wafer section (fig. 26), located just above the tip of the vent tube, was removed to provide a specimen for burnup analysis.

Fuel burnup determinations were made by mass spectrometric measurements of uranium, plutonium, and fission-product neodymium isotopes. Two samples of fuel were analyzed, one from the side towards the peak flux and the other 180° away from peak flux. The analyses were made according to ASTM Method E321, and the burnup calculations were made using the GE-NONPRO code which is similar to that described in GEAP-5355 (ref. 9).

The results are shown in table XIV. The "best value" for the average burnup is 0.644 atom percent fission (based on total uranium atoms present before irradiation), 1516×10^{20} fissions per cubic centimeter of fuel, or 3.94 atom percent fission (based on ^{235}U atoms originally present). This agrees quite well with the burnup inferred from the operating history (1.453×10^{20} fissions/cm^3).

The burnup values in table XIV are based on both neodymium and heavy-element isotopic measurements. The neodymium burnup values are considered more reliable than the heavy-element values since they do not depend on the measurement of a relatively small change in the uranium-235 concentration. However, the heavy-element burnup values do provide an independent check. As expected, an asymmetry of about 5 percent in burnup was found between the fuel on the side toward peak flux and the backside of the specimen.

DISCUSSION OF RESULTS

As given in the INTRODUCTION, the modified objectives of this experiment were to

(1) Study structural integrity and fuel-clad compatibility

(2) Determine central vent effectiveness

(3) Study the effect of thermal cycling on clad swelling

(4) Life test to a burnup of 4×10^{20} fissions per cubic centimeter at a maximum clad temperature of 1690° C

(5) Study fuel redistribution.

The degree to which these objectives were met is discussed in this section.

Inpile Operation

Figures 6 and 7 show the fuel condition before and after the 190-hour redistribution period. Figure 7 shows the fuel completely redistributed in a layer of constant thickness at the wall. The fin effect of the central vent caused the fuel to build up along its length. Although the definition of the radiograph does not allow direct measurement, the fuel appears to extend about two-thirds of the vent length. This is in excellent agreement with the calculated amount of 70 percent. The 190 hours establishes only an upper limit to the redistribution time period. The actual value may have been considerably less.

A thorough discussion of the thermal cycling results is given in reference 10 and will not be repeated here except in summary. Fifty 30-minute thermal cycles between the maximum cladding temperatures of 847° and 1690° C had no measurable effect on either the fuel or capsule structure. Another set of 24 thermal cycles was run between maximum cladding temperatures of 467° and 1690° C, with a 10-hour hold at the high temperature. Radiography showed only slight (0.007 to 0.012 cm, max.) downward bowing of the end cap, but no radial swelling of the cladding.

These results, along with a comparison of the results with those of the previously run capsules, indicate that thermal cycling is not a major cause of fuel swelling.

Table XV lists life test parameters. Life testing conditions of 500 watts per cubic centimeter fission power and a maximum clad temperature of 1690° C were maintained for 2607 hours. During that period the capsule underwent seven fast setbacks or scrams and 92 normal insertion-withdrawals for a total of 99 thermal cycles. Failure occurred sometime before 2607 hours when the bottom end cap and clad failed circumferentially at the weld. Measurements of the radiography after the fact reveal that the vent tube probably separated from the end cap during thermal cycling. Apparently, the redistributed fuel kept the vent tube in its position relative to the top end cap while the bottom end cap was strained downward (fig. 50).

Dimensional Stability

The maximum distortion of the side wall was measured as a 0.015-centimeter (0.006-in.) growth in diameter. The bottom end cap was deformed and eventually failed at the weld where the end cap was joined to the cladding. Whether the diametral growth would have been greater if the bottom cap had not deformed is an open question.

Structural Integrity

Metallographic examination of longitudinal sections of the fuel specimen revealed defects and/or failures in the tungsten cladding at two points in the side wall (figs. 33 and 34), at the weld joints at both the top and bottom end caps (figs. 31 and 47), and at the joint between the stem tube and the top end cap (fig. 30).

The defects observed in the side-wall-cladding were intergranular cracks, partially or fully penetrating the 0.101-centimeter (0.040-in.) thick tungsten wall. Major structural failures occurred in the weld joints between the CVD W cladding sleeve and the arc-cast tungsten end caps. The bottom end cap was dished sufficiently to impose stresses on the weld joint to the point of failure. However, neither the arc-cast tungsten or the CVD W cladding showed any indications of brittle fracture. The top cap was joined to the side cladding by a series of spike welds and initiation of cracks was observed in the weld zone but not to the point of failure of the side cladding. The top end cap was severely cracked under the thermocouple well and adjacent to the brazed joint between the stem tube and the end cap. This may have occurred during brazing as a result of thermal stresses.

The fracture of the central vent tube was an unexpected finding and, with all the data available from metallographic examination, cannot be adequately explained. During assembly of the fuel specimens for this experiment, the central vent tubes presented some problems. Two of the CVD W tubes were broken in efforts to enlarge the hole at one end, and one was broken when it was being removed from the fixture after welding it to the bottom end cap. Electron-beam welds were made both inside and outside the end cap; this caused two brittle heat-affected zones in the vent tube. It is possible that the tube was cracked at the inside weld before irradiation and fractured some time after redistribution of fuel had been completed.

Gross failure occurred in weld areas and these appeared to have resulted from deformation stresses on the weld joint itself. Alternate joint designs might have prevented weld failures if the deformation had been anticipated. Also, the development of electron-beam welding procedures for joining materials with dissimilar microstructures (CVD W against arc-cast tungsten) to provide a homogeneous weld structure should be considered to maintain joint integrity.

It should be noted that the structural integrity of the molybdenum-rhenium brazed joint between the CVD W-Re stem tube and the top end cap was excellent. Complete joint penetration by the braze material was achieved and compatibility with the two types of microstructures was good. This suggests that where operating temperatures permit brazing should be considered for joining tungsten cladding components of the fueled specimen assembly.

Tungsten-Uranium Dioxide

Compatibility of UO_2 with both the arc-cast tungsten end caps and the CVD W cladding appeared to be good. There were no precipitates or foreign phases in the grain-boundaries of the tungsten that could be attributed to fuel reaction. In the weld areas that failed or ruptured, the cause appeared to be mechanical interaction rather than chemical reaction with the fuel.

Vent Tube Effectiveness

All thermionic reactor designs with a lifetime in excess of 1 year provide for venting gaseous fission products from the fuel specimen to external regions where they can be accommodated (ref. 8). If the fuel structure is impermeable so as to prevent escape of fission gases to the fuel exterior, a central vent must be employed. The central vent in experiment 66-03-2 consisted of a tube inserted through the specimen end cap to directly bleed fission gases from the central cavity. This tube was machined to a 0.127-centimeter (0.050-in.) outside diameter and had a bore diameter of 0.025 centimeter (0.010 in.). The length was about 1.27 centimeters (0.5 in.) so the tip was in the upper half of the fuel cavity (fig. 1).

Wilkins (ref. 8) performed parametric studies on this vent design for three values of fission gas pressure and concluded that acceptable UO_2 loss rates and fission-gas pressure differential across the vent tube would be achieved. A gas pressure differential of 10 torr was considered adequate to drive the fission gasses through the vent under all pressure conditions studied. Wilkins concluded that the central vent of experiment 66-03-2 was sized appropriately to accomplish its design objectives. The UO_2 loss rates were predicted as not in excess of 0.33 milligram per year.

Krypton and Xenon[1] found in the cover gas indicated that fission gas could have escaped through the vent tube or the failed bottom end-cap joint or both. It was concluded

[1]Analysis showed that 60 percent of Kr and 40 percent of Xe produced in the fuel escaped into the cover gas surrounding the fuel specimen.

that the vent effectiveness in releasing fission gases could not be determined because of the condition of the vent tube and fuel specimen.

Analysis of the deposit on the catcher plate below the central vent showed that 5.8 milligrams of UO_2 along with solid fission products such as cerium-144 were lost from the fuel cavity. Based on the thermal condition, the solid products could have escaped as vapor.

Disposition of Fission Products

As shown in table IX(c), over 60 percent of the calculated krypton production and over 40 percent of the calculated xenon production were found in the gas surrounding the vented fuel specimen. It is believed that the actual amount of krypton and xenon released from the fuel was higher. The charcoal in the gas sample bottle was used to insure that all of the gases removed from the capsule would be trapped. However, the technique used to remove the small sample from the bottle for analysis may not have separated the adsorbed gases from the charcoal. The sample bottle was heated to (360° C), at which temperature the xenon and krypton are not held by the charcoal, but, since no gas flow was employed, the amount actually released depended solely on the achievement of a thermodynamic equilibrium. Thus, some of these gases may have remained on the charcoal. In any case, the analysis showed that a large fraction of these gases did escape, which is consistent with the known properties of UO_2 fuel.

The gross gamma scan of the steel containment can and fuel specimen indicated that condensable fission products migrated from the fuel, through the vent tube (or through the end-plate rupture) and were deposited on the catcher plate and in the lower end of the containment can. Some accumulation of fission products was also indicated on the walls of the upper part of the containment can. The finding of a relatively large amount (5.8 mg) of UO_2 on the catcher plate would indicate that considerable amounts of solid fission products also escaped from the fuel specimen to the atmosphere of the containment can.

Uranium Dioxide Fuel Redistribution

Examination of both transverse and longitudinal sections of the clad fuel specimen revealed that complete redistribution of UO_2 fuel had occurred. The fuel structure was similar to that of the specimens of experiment 66-03-1 (ref. 3), which operated at a similar specimen surface temperature (1650° C). The structure was composed of columnar grains and lenticular pores migrating to the center. Fission gas bubbles were

collected in the grain boundaries. A layer of fine-grain fuel encircled the outer periphery of the fuel pellet where a high-temperature gradient existed and condensation of UO_2 vapors occurred at the cooler cladding wall. Small metallic particles in the UO_2 at the central cavity were assumed to be solid fission products or impurities in the fuel.

A relatively large accumulation of metallic impurities was found at the bottom end-cap where the vent tube had fractured and analysis of this second phase material by X-ray fluorescence identified the elements iron, nickel, tungsten, and uranium. The iron and nickel were traced to the UO_2 pellet and the CVD W vent tube in the pretest condition. During irradiation the fuel temperature exceeded the melting point of iron, nickel, and uranium, causing these elements to alloy with tungsten. This material then appeared as second-phase impurity in the redistributed fuel.

The analysis of the deposit on the catcher plate below the vent showed that a total of 5.8 milligrams of UO_2 escaped from the emitter specimen, which is more than 60 times the fuel loss through the central vent tube that was predicted by Wilkins. However, this high loss is attributed to the rupture in the bottom end plate weld, which allowed fuel and fission products to escape. In view of this failure of the end plate and the fracture of the vent tube, no conclusions can be drawn as to the actual fuel loss through the central vent tube.

CONCLUDING REMARKS

Experiment 66-03-2 had an average burnup of 1.5×10^{20} fissions per cubic centimeter over an operating period of 2607 hours. The calculated average cladding temperature during this operating period was 1650° C. A maximum possible 0.015-centimeter (0.006-in.) diametral growth of the 0.101-centimeter (0.040-in.) thick chemically vapor deposited tungsten cladding was observed during the postirradiation examination. Whether this diametral growth would have been greater if the bottom cap had not deformed is open to question. The uranium dioxide fuel and chemically vapor deposited tungsten cladding were found compatible after the fuel specimen was subjected to the operating conditions.

The failure of the bottom end cap weld joint indicates a need for redesign of the end cap joint to cladding sleeve. This redesign should consider the shrinkage that occurs in an electron-beam weld joint and the stresses imposed by the redistributed fuel during thermal cycling. The fracture of the central vent tube could not be completely analyzed from the posttest findings. A shorter tube might be as effective in venting the fuel and would be less fragile. The stem tube, which broke during irradiation of this experiment, should be fabricated of wrought tungsten - 25-weight-percent rhenium tubing, which

would have better ductility than the chemically vapor deposited tungsten tubing used in this specimen.

Lewis Research Center,
National Aeronautics and Space Administration,
Cleveland, Ohio, October 27, 1972,
112-27.

REFERENCES

1. Gregory, T. L.; Boyle, R. F.; and Danko, J. C.: Irradiation of UO_2 Fuel Clad with Tungsten-25 w/o Rhenium. Rep. GEST-2100, General Electric Co. (NASA CR-72356), Dec. 1967.
2. Rosicky, E.; Danko, J. C.; and Lloyd, W. R.: Additional Radioactive Materials Laboratory Experimental and Analytical Investigations for Support of a UO_2 Irradiation - A supplement to NASA CR-72356. Rep. GESP-9010, General Electric Co. (NASA CR-72721), Dec. 1969.
3. Allen, D. C.; and Titus, G. W.: Irradiation of UO_2 Fuel Clad with Chemically Vapor Deposited Tungsten Operation and Post Irradiation Examination. Rep. GESP-9017, General Electric Co. (NASA CR-72988), Oct. 1970.
4. Gregory, T. L.; and Allen, D. C.: Design, Fabrication and Installation of Capsule for Irradiation of UO_2 Fuel Clad with Tungsten. Rep. GESP-9002, General Electric Co. (NASA CR-72688), Feb. 1970.
5. Henderson, W. B.: Program Chains (NMP-856). Rep. GEMP-490, General Electric Co., Mar. 1967.
6. Walker, W. H.: Fission Product Data for Thermal Reactors. Part 1 - Cross Sections. Rep. AECL-3037, Atomic Energy of Canada, Ltd., Dec. 1969.
7. Templin, L. J., ed.: Reactor Physics Constants. Second ed. Rep. ANξ-5800, Argonne National Lab., July 1963.
8. Wilkins, D. R.; and Duderstadt, E. C.: Performance Studies of a Centrally-Vented Fuel Form for Nuclear Thermionic Converter Applications. Rep. GESP-9016, General Electric Co. (NASA CR-72788), July 1970.
9. Rider, B. F.; Ruiz, C. P.; Peterson, J. P., Jr.; and Smith, E. R.: Burnup: A Fortran IV Code for Computing U and Pu Burnup From U, Pu, and Nd Mass Spectrometric Measurements. Rep. GEAP-5355, General Electric Co., Mar. 1, 1967.

10. deBogdan, Claude E.: Effect of Thermal Cycling During Irradiation of Vented Tungsten-Clad Uranium Dioxide Fuel Specimens. NASA TM X-2252, 1971.

TABLE I. - CHEMICAL ANALYSES OF URANIUM DIOXIDE FUEL PELLET AFTER FINAL HYDROGEN FIRING

Element	Amount detected, ppm
Emission spectrographic analysis	
Al	<4
Bi	<1
B	1
Ca	<30
Cd	<.5
Cr	14
Co	<2
Cu	2
Fe	25
Pb	<1
Li	<5
Mg	5
Mn	.1
Mo	<6
Ni	65
Si	90
Ag	<.1
Na	<40
Sn	<1
V	<11
Zn	<50
Fe+Ni+Fe	104
Chemical analysis	
C	8
Cl	<5
F	3

Thermogravimetric oxygen to uranium ratio	2.010±0.005
Coulometric oxygen to uranium ratio	2.0014±0.0009

Isotopic analysis		
Uranium isotope	Weight percent	Standard deviation, percent
234	0.180	±0.002
235	16.19	±.07
236	.027	±.003
238	83.603	±.070

TABLE II. - CHEMICAL ANALYSIS OF CHEMICALLY VAPOR DEPOSITED TUNGSTEN TUBING USED FOR CLADDING

Element	Vendor analysis, ppm
C	17
Fl	7
H_2	.1
O_2	3.1
N_2	.3
Al	2
Cu	<.3
Fe	<2.1
Si	8
Mn	<.5
W	Balance

TABLE III. - CHEMICAL ANALYSIS OF VACUUM ARC-CAST TUNGSTEN ROD USED FOR EMITTER END CAPS

[Tungsten content, 99.9 percent.]

Element	Vendor analysis, ppm	GE analysis, ppm
C	<5	29
O	2	17
N	3	14
H	<1	<1
Fe	12	60
Ni	<1	<1
Si	<20	<20
Mo	20	<20

TABLE IV. - CHEMICAL ANALYSIS OF CHEMICALLY VAPOR DEPOSITED TUNGSTEN TUBING USED FOR CENTRAL VENT

Element	Vendor analysis, ppm
C	7.0
O	5.8
N	2.0
F	13.0
H	.8
Fe	~170
Al	<.5
Cu	<.3
Ni	6.3
Si	5.4

TABLE V. - CHEMICAL ANALYSIS OF CHEMICALLY VAPOR DEPOSITED TUNGSTEN-22 WEIGHT PERCENT RHENIUM TUBING USED FOR STEM

Element	Vendor analysis, ppm	Check analysis, ppm
C	16	10
O	32	40
N	2.6	30
F	8	-----
H	.9	.5
Fe	----	20
Si	----	<20

TABLE VI. - ANALYSIS OF CAPSULE FILL GAS FOR EXPERIMENT 66-03-2

Gas	Sample 1, vol. % (a)	Sample 2, vol. % (a)	Average samples 1 and 2, vol. %
He	41.23	38.96	40.4
Ar	53.49	57.19	55.3
N	5.10	3.47	4.3
O	.20	.31	.25
CO_2	.03	.04	.035
H_2O	Trace	Trace	Trace

[a]Analysis given is average of three analyses of each sample. Analysis performed by Stanford Research Institute (SRI).

TABLE VII. - CAPSULE OPERATING HISTORY

Reactor cycle	Date completed	Accumulated hours at temperature	Total burnup fiss/cm^3×10^{-20}	Total thermal cycles	Remarks
97	10-13-69	----	-----	--	Attempted to reach temperature observed over large temperature differences - pulled to radiograph
98	11-3-69	----	-----	--	Radiograph (fig. 7) showed leaking (30 mil) specimen capsule
99	11-19-69	----	-----	--	Removal of (30 mil) specimen
100	12-9-69	----	-----	--	Removal of (30 mil) specimen
101	12-24-69	----	-----	--	Radiograph post fix, showed (40 mil) specimen to be r
102	1-15-70	----	-----	--	No testing
103	2-8-70	190	0.106	4	
104	3-1-70	----	-----	--	Radiograph (fig. 8) showed redistribution complete
105	3-23-70	191	0.106	54	Short thermal cycles (see fig. 9)
106	4-10-70	----	-----	--	Radiographs showed no change
107	5-18-70	194	0.106	60	No testing due to low-flux, thermocouple noise
108	6-5-70	410	0.229	85	Long thermal cycles (see fig. 10)
109	6-22-70	----	-----	--	Radiograph (fig. 11) showed bottom end cap dished ~(5 mil); no radial swelling; lead tube bent after radiograph, straightened in hot lab
110	7-9-70	634	0.356	86	
111	7-27-70	----	-----	--	Radiograph (fig. 12) showed broken stem; specimen shifted downward ~0.5 mm
112	8-17-70	1005	0.565	87	Shifted to constant power operation
113	9-8-70	1424	0.795	92	
114	9-28-70	1554	0.868	94	Retracted 9-16-70 for radiographs
115	10-21-70	----	-----	--	Radiograph (fig. 13) showed specimen now bottomed; bottom end cap dished (~15 mils)
116	11-8-70	1909	1.064	95	
117	12-1-70	2228	1.241	97	
118	12-18-70	2607	1.453	99	
119	1-18-70	----	-----	--	Radiograph (fig. 14) showed bottom end cap and clad failed at weld
120	1-30-71	----	-----	--	Radiographs taken 45^o counterclockwise of 275 and at 45^o clockwise of 275 showed no failure

TABLE VIII. - RESULTS OF FLUX WIRE ANALYSIS

(a) Thermal neutron fluences; aluminum-cobalt wires

	Count rate for ^{60}Co/gm Co, dis/sec	Fluence,[a] neutrons/cm^2	Average flux,[b] nv, neutrons/sec-cm^2
Towards peak flux	3.07×10^{11}	1.9×10^{20}	2.0×10^{13}
180° from peak flux	2.25×10^{11}	1.4×10^{20}	1.5×10^{13}

(b) Fast neutron fluences; stainless steel wires

	Count rate for 54 Mn/gm Fe	Fluence,[c] neutrons/cm^2	Average flux,[b] nv, neutrons/sec-cm^2
Towards peak flux	1.16×10^{7}	1.5×10^{19}	1.6×10^{12}
180° from peak flux	8.65×10^{6}	1.1×10^{19}	1.2×10^{12}

[a]Wavelength, 2200 m/sec.

[b]Based on operating for 2607 hr.

[c]Energy level, >1 MeV.

TABLE IX. - RESULTS OF GAS ANALYSIS

(a) Gas analysis after irradiation

	Volume measured[a] reduced to STP[b]	Percent volume[a] measured excluding CO_2
AR	1.956 cm^3	54.2
He	.544 cm^3	15.06
N	.181 cm^3	5.02
Kr	.146 cm^3	4.04
Xe	.673 cm^3	18.65
H	.100 cm^3	2.76
H_2O	---------	-----
CH_4	.011 cm^3	.30
Ne	<60 ppm	-----
O_2	<40 ppm	-----
CO	<40 ppm	-----
^{85}Kr	2.87×10^{17} atoms	-----
^{133}Xe	Not detected	-----
Total gas volume	9.8 cm^3	-----

(b) Comparison of SRI gas analysis results before irradiation with vellecitos results of post irradiation analysis

	Average SRI preirradiation analysis, volume percent	Post irradiation[a, c] analysis, volume percent
AR	55.3	73.1
He	40.1	20.3
N	4.3	6.6

(c) Comparison of fission gases found in gas sample with calculated volumes based on fuel burnup

	Measured volume reduced[a, c] to STP	Calculated volume base on fuel burnup
Kr	0.146 cm^3	0.232 cm^3
Xe	.673 cm^3	1.569 cm^3
^{85}Kr	2.87×10^{17} atoms	4.43×10^{17} atoms

[a]Accuracy ±5 percent.

[b]Standard temperature and pressure.

[c]Corrected for He, AR, and N_2 from postirradiation gas analysis excluding CO_2.

TABLE X. - ISOTOPIC YIELDS USED FOR ANALYSIS

Isotope	Fission yield,[a] percent	Capture cross section, b	Half life	Comments
^{83}Kr	0.544	220	∞	Capture goes to ^{84}Kr
^{84}Kr	1.00	.14	∞	
^{85}Kr	.281	<15	10.76 yr	Calculated by CHAINS (ref. 5)
^{85}Kr	2.02	.06	∞	
^{87}Kr	.002	<600	78 min	Equilibrium yield
^{88}Kr	.005	-------	2.8 hr	Equilibrium yield
89Kr	.0001	-------	3.2 min	Equilibrium yield
Total Kr	3.85	-------	-------	----------
^{131}Xe	2.93	110	∞	Capture goes to ^{132}Xe
^{132}Xe	4.38	.25	∞	
^{133}Xe	.46	-------	5.27 day	Equilibrium yield
^{134}Xe	8.06	.23	∞	
^{135}Xe	.0095	3.6×10^{6}	9.2 hr	Calculated by CHAINS (ref. 5)
^{136}Xe	6.46	.28	∞	*Direct production*
^{136}Xe	4.13	.28	∞	Calculated from ^{135}Xe capture
^{137}Xe	.0002	-------	3.9 min	Equilibrium yield
^{138}Xe	.0009	-------	17 min	Equilibrium yield
Total Xe	26.43	-------	-------	----------

[a]All yields are calculated for end of irradiations. Short-lived isotopes are equilibrium values at end of irradiation.

TABLE XI. - DIAMETRAL MEASUREMENTS OF FUEL SPECIMEN OF EXPERIMENT 66-03-2

[Original diameter of tungsten cladding sleeve as-fabricated, 1.1821 cm (0.4654 in.).]

Diameter designation	Diameters 0^{o} to peak flux		Diameters 90^{o} to peak flux	
	cm	in.	cm	in.
A, bottom end shroud	1.1917 to 1.1945	0.4692 to 0.4703	1.1869 to 1.1828	0.4673 to 0.4657
B, bottom end cap	1.1955 to 1.1912	.4707 to 0.4690	1.1902 to 1.1892	.4686 to 0.4682
C, fuel	1.1905 to 1.1899	.4687 to 0.4685	1.1917 to 1.1895	.4692 to 0.4684
D, fuel	1.1955 to 1.1897	.4807 to 0.4684	1.1912 to 1.1897	.4690 to 0.4684
E, fuel	1.1973 to 1.1920	.4714 to 0.4693	1.1922 to 1.1887	.4694 to 0.4680
F, fuel	1.1973 to 1.1973	.4714 to 0.4714	1.1927 to 1.1938	.4696 to 0.4700
G, fuel	1.1953 to 1.1971	.4706 to 0.4713	1.1930 to 1.1920	.4697 to 0.4693
H, top end cap over weld	1.1907 to 1.1902	.4688 to 0.4686	1.1910 to 1.1895	.4689 to 0.4683

TABLE XII. - COMPOSITION OF

DEPOSIT ON CATCHER PLATE

Material	Quantity
^{235}U	0.855 mg
^{238}U	4.93 mg
^{141}Ce	.33 m Ci
^{144}Ce	3.1 m Ci
^{95}Nb	3.6 m Ci
^{95}Zr	2.0 m Ci

TABLE XIII. - POSTIRRADIATION ISOTOPIC

COMPOSITION AND BURNUP

Item	Pretest	Sample at 0°	Sample at 180°
Isotopic composition, at. %			
^{234}U	0.18	0.182	0.357
^{235}U	16.19	15.79	15.73
^{236}U	.027	.140	.148
^{238}U	83.603	83.889	83.767
^{239}Pu	------	98.41	97.40
^{240}Pu	------	1.53	2.18
^{241}Pu	------	.06	.28
^{242}Pu	------	.0005	.14
Atom ratio, $^{239}Pu/^{238}U$	------	2.62×10^{-4}	2.99×10^{-4}
Fissions, at. %, from -			
^{235}U	------	0.566	0.600
^{239}Pu	------	6.7×10^{-4}	1.8×10^{-3}
^{241}Pu	------	2.7×10^{-6}	7.9×10^{-5}
^{238}U	------	0.033	0.600
Total fissions, at. %	------	0.589	.638
Fissions per cubic centimeter (by heavy element)	------	1.386×10^{20}	1.501×10^{20}
Fissions, at. %, from -			
^{148}Nd	------	0.603	0.664
^{145}Nd	------	.620	.684
^{146}Nd	------	.617	.675
Average fissions from Nd	------	.613	.674
Fissions per cubic centimeter (by Nd)	------	1.442×10^{20}	1.586×10^{20}

[a]Based on total uranium atoms before irradiation.

TABLE XIV. - LIFE TEST PARAMETERS

Fission power, W/cm^2	500
Maximum clad temperature, ^{o}C	1690
Time at temperature, hr	2607
Number of thermal cycles	99
Burnup (calculated), fissions/cm^3	1.5×10^{20}
Burnup (calculated, at. %	0.54

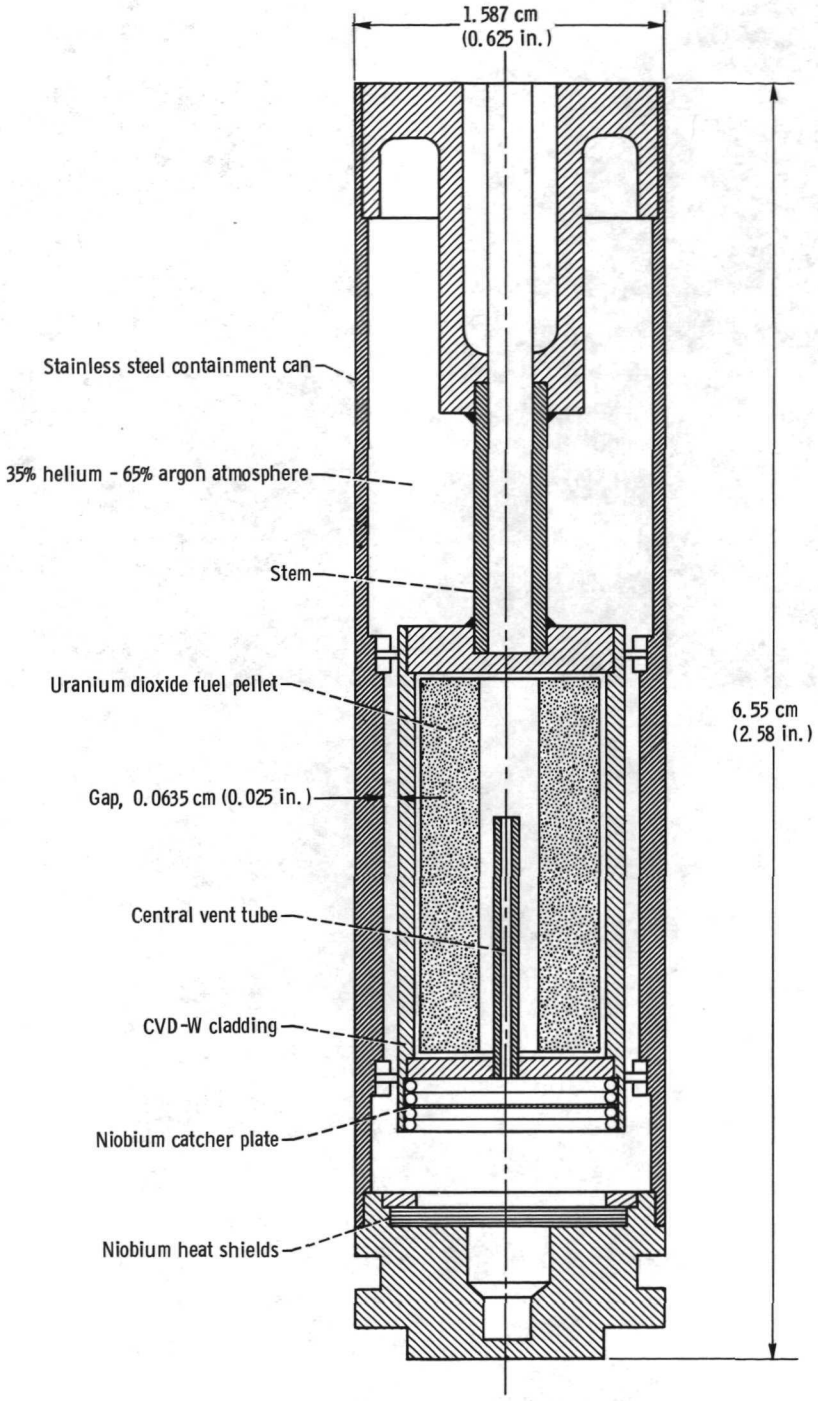

Figure 1. - Fuel specimen and containment can assembly for experiment 66-03-2.

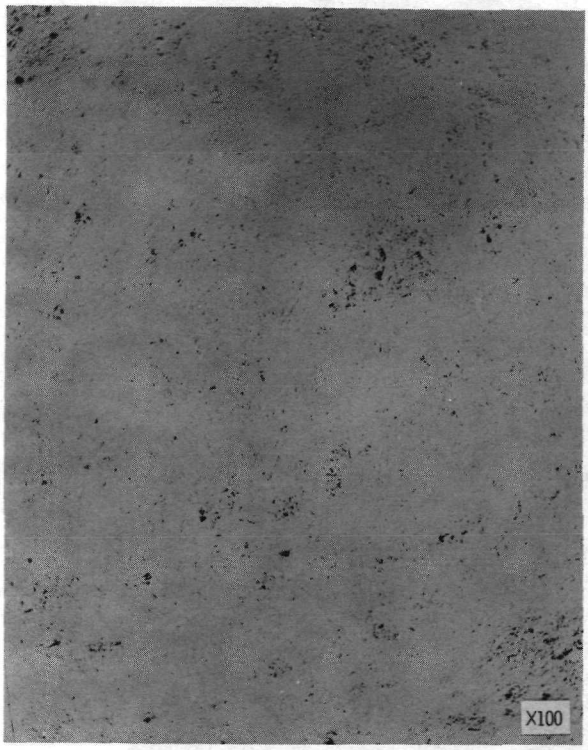

Unetched

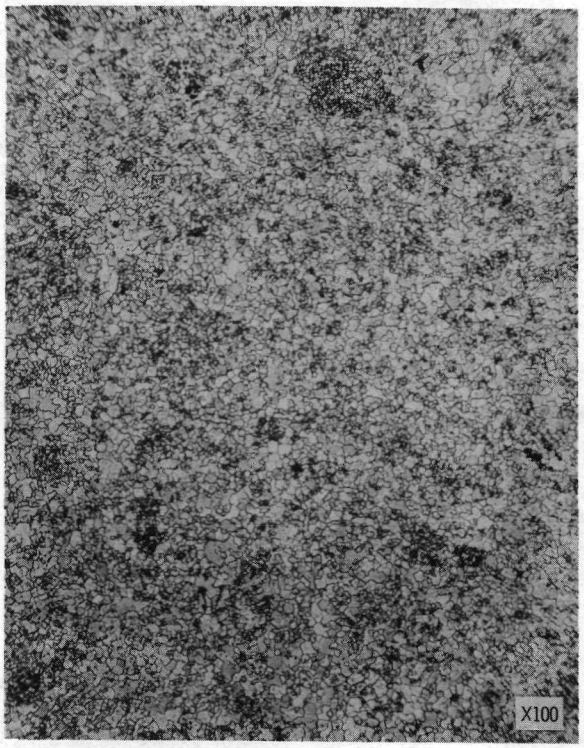

Etched

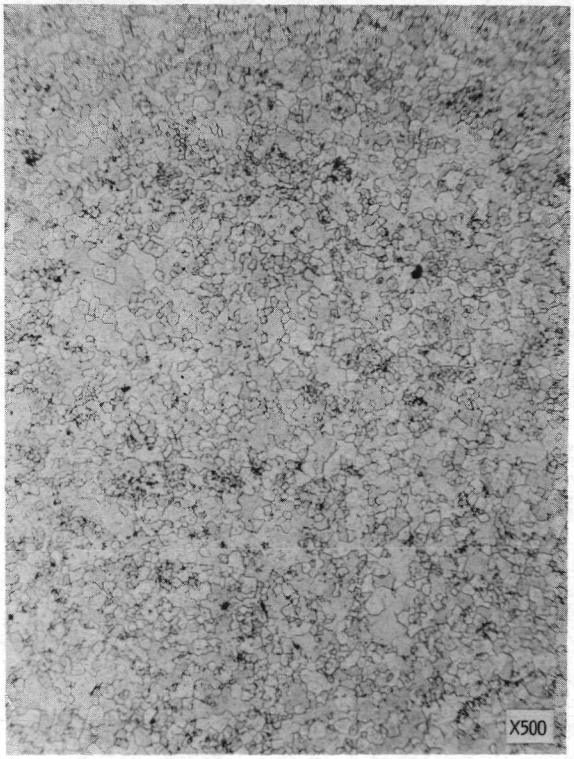

Unetched

Figure 2. - Microstructures of uranium dioxide fuel pellets after vacuum firing at 1800° C for 30 minutes. (Reduced 8 percent in printing.)

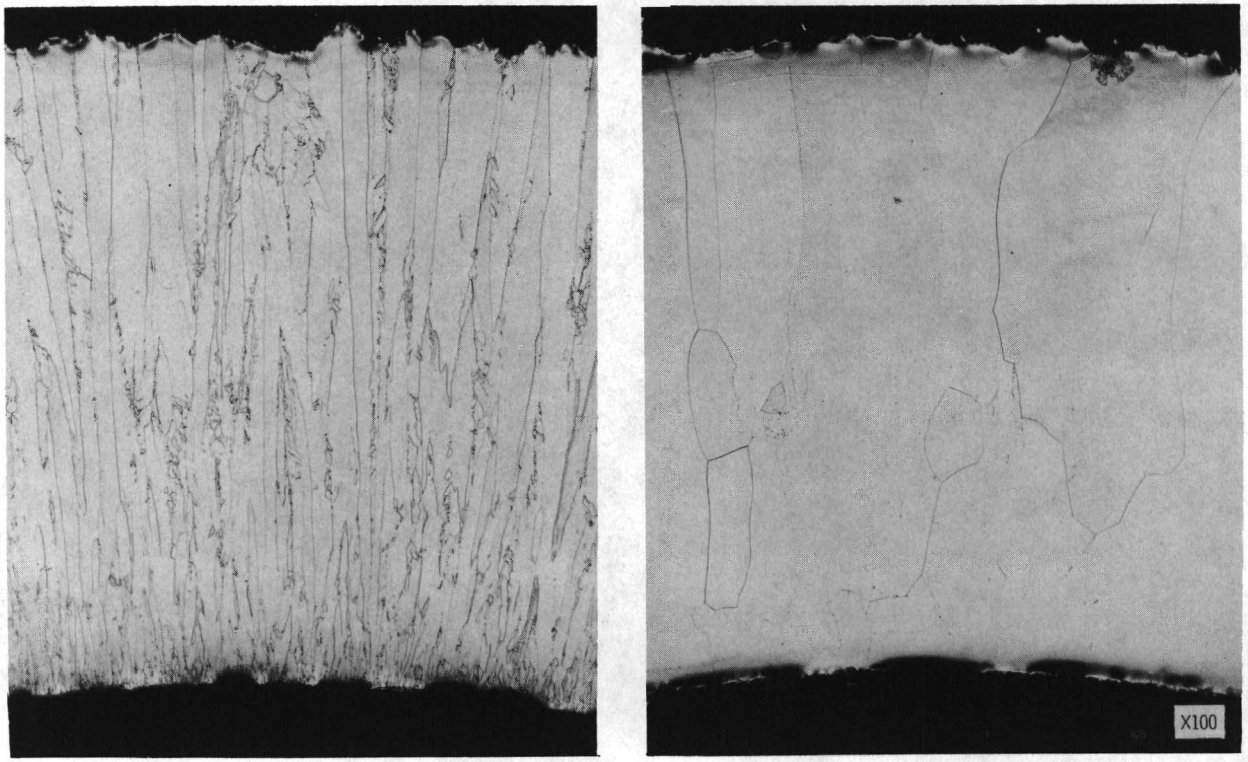

As-received

After 2500° C test

Figure 3. - Microstructures of 0.1016-centimeter (0.040-in.) wall of chemically vapor deposited tubing in as-received condition and after 2500° C swelling test. (Reduced 8 percent in printing.)

As-received

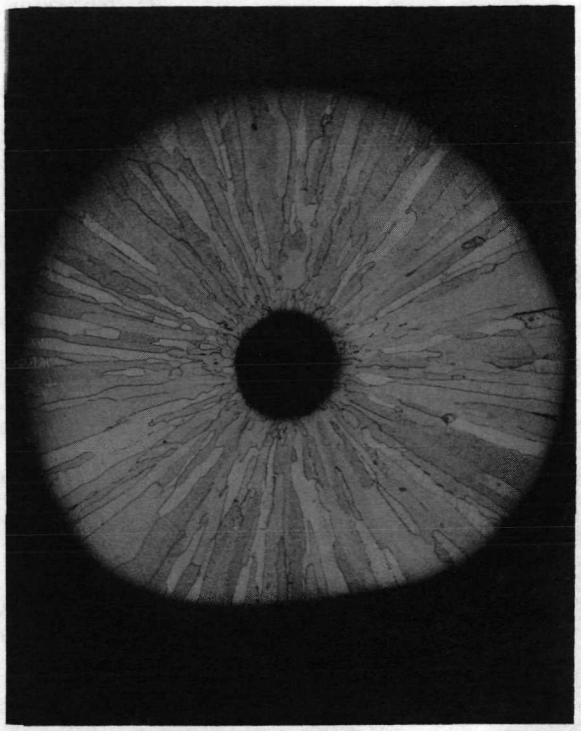

After 2000° C for 2 hours

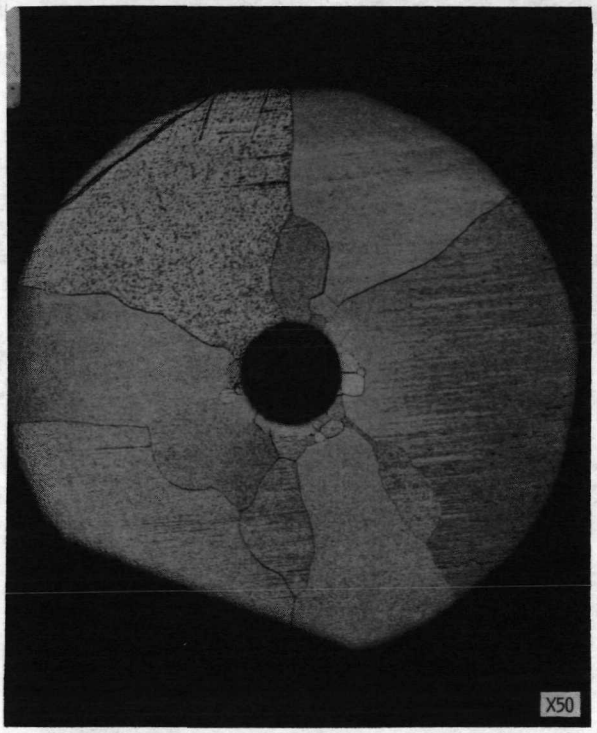

After 2500° C, 1-hour swelling test

Figure 4. - Microstructures of chemically vapor deposited tungsten tube used for central vent tube. (Reduced 17 percent in printing.)

As-received

After 2000° C, 2-hour homogenization

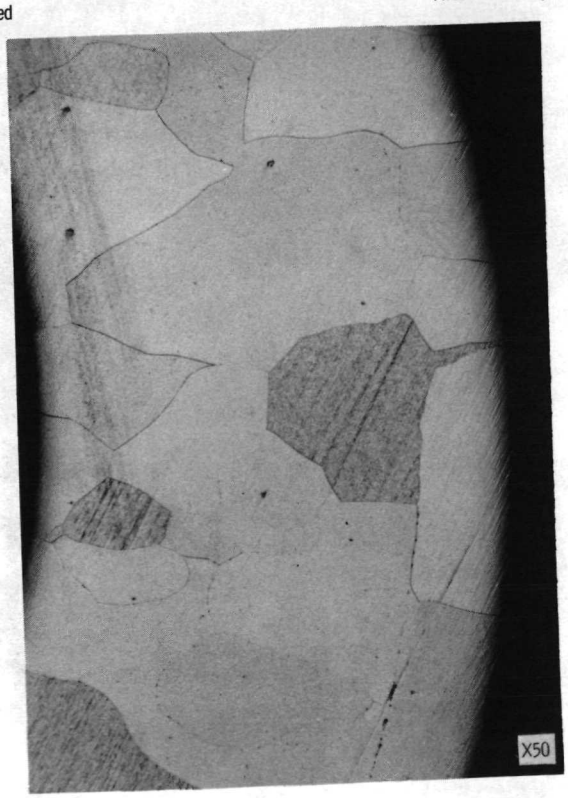

After 2500° C, 1-hour swelling test

Figure 5. - Microstructures of chemically vapor deposited tungsten - 25-weinght-percent rhenium tubing used for stem. (Reduced 10 percent in printing.)

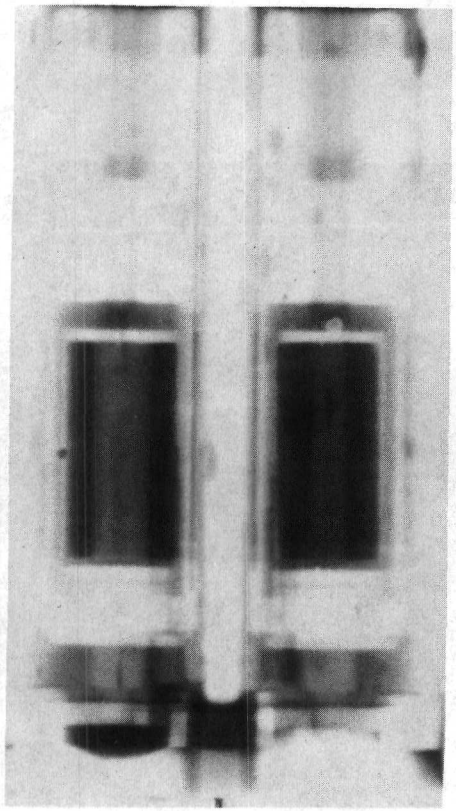

Figure 6. - Preirradiation neutron radiograph.

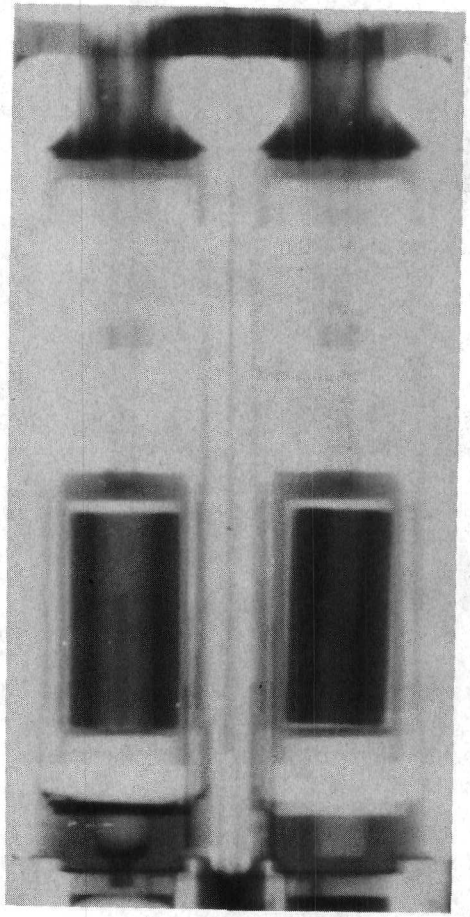

Figure 7. - Radiograph showing water in .75 millimeter (30 mil) capsule.

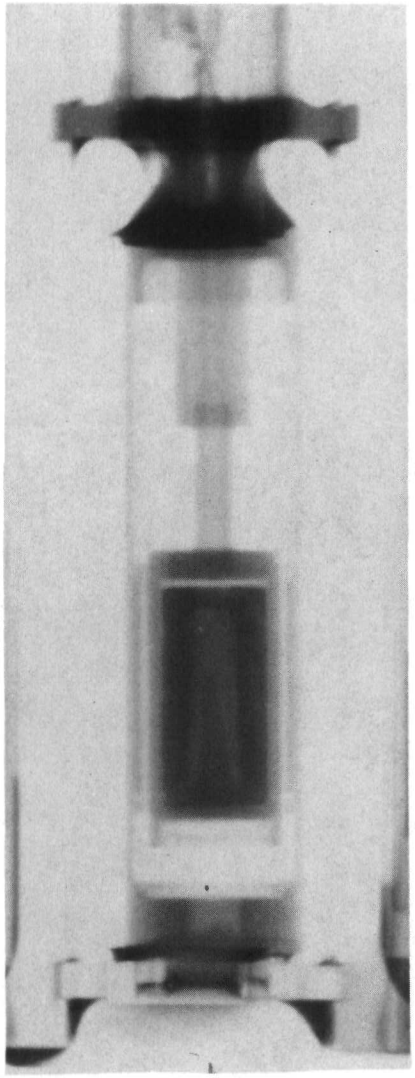

Figure 8. - Fuel redistribution after 190 hours.

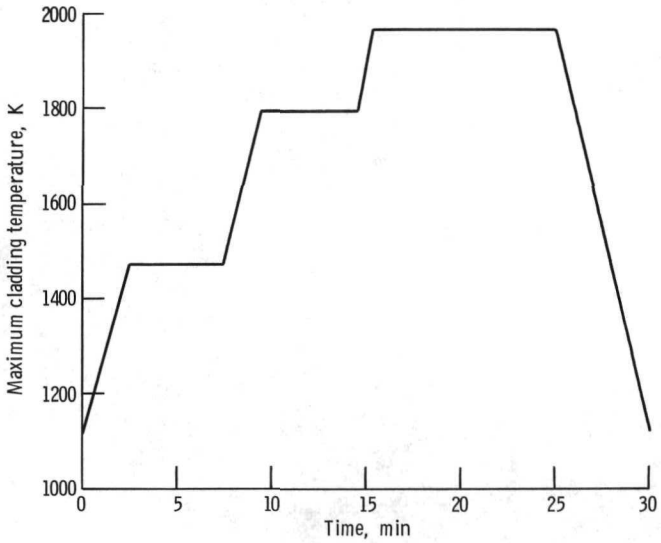

Figure 9. - Typical short cycle; experiment 66-03-2.

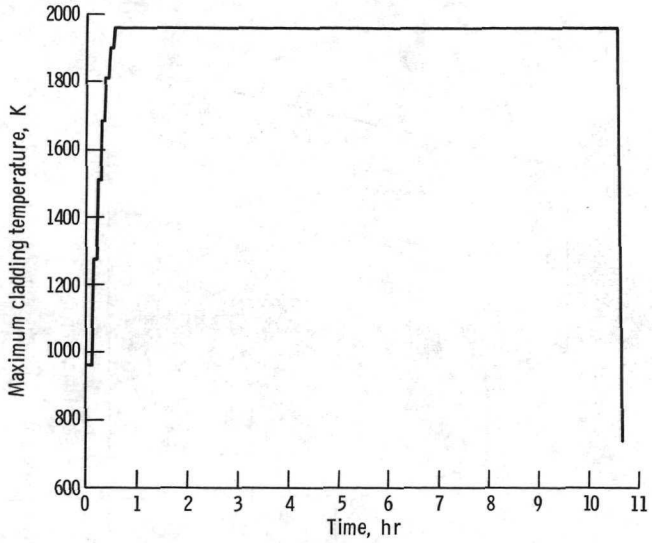

Figure 10. - Typical long cycle; experiment 66-03-02.

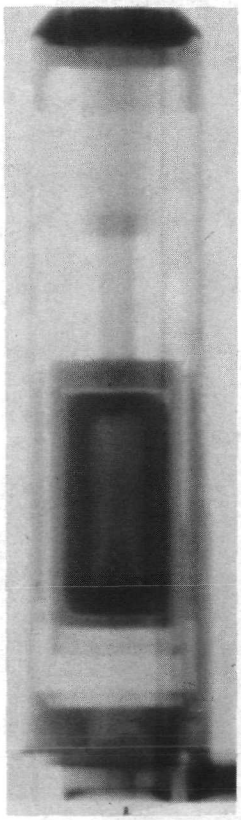

Figure 11. - Specimen condition after 24 long (10 hour) thermal cycles.

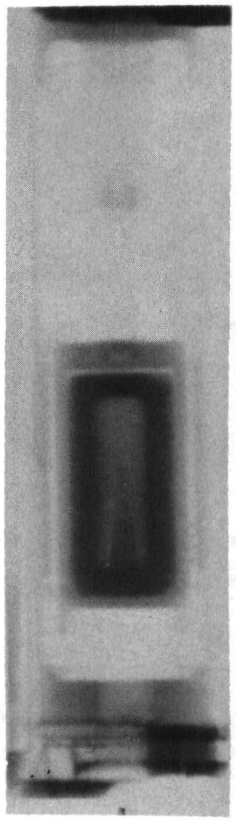

Figure 12. - Radiograph showing broken stem.

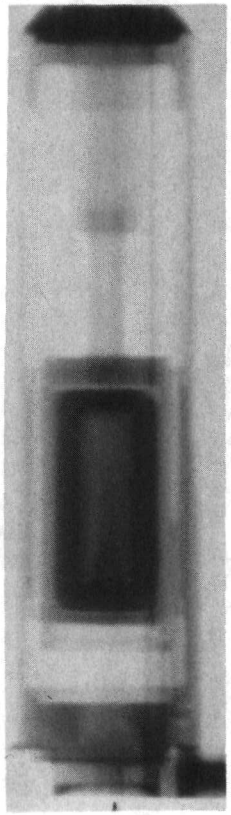

Figure 13. - Bottomed specimen.

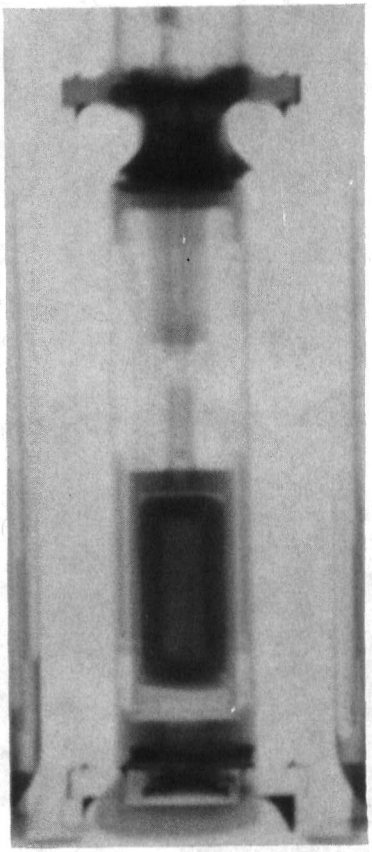

Figure 14. - Bottom end cap failure.

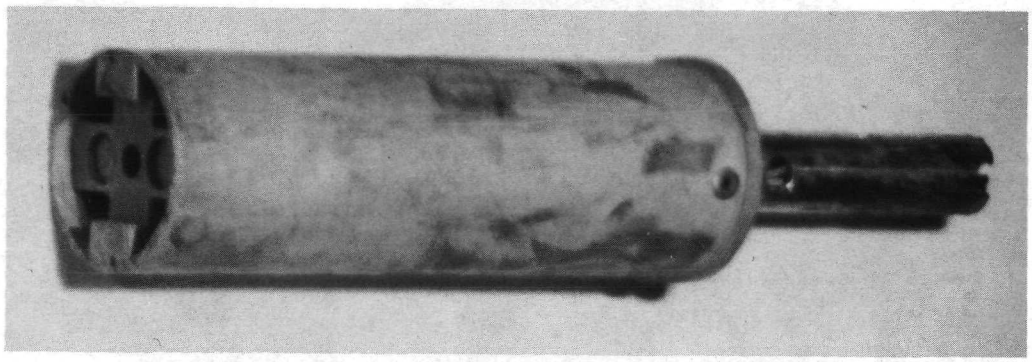

Figure 15. - Condition of experiment 66-03-2 capsule upon arrival in hot cell.

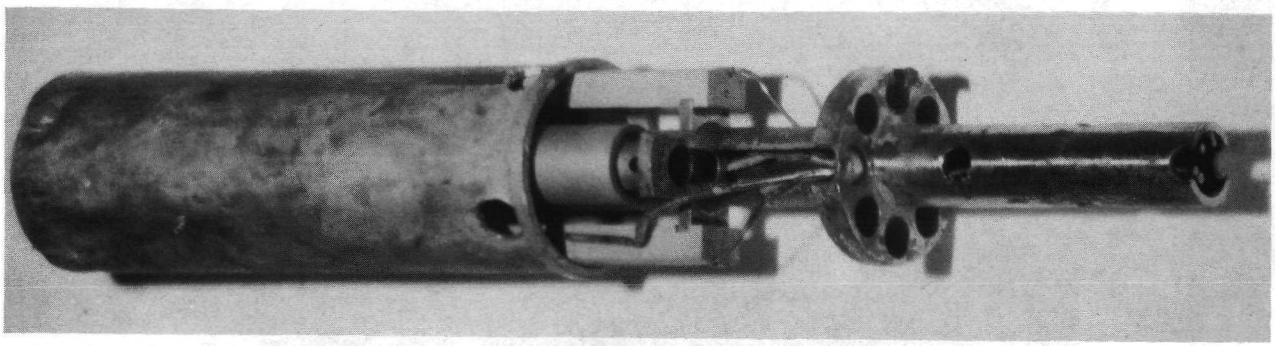

Figure 16. - Removal of capsule fixture from outer shroud after drilling out rivets.

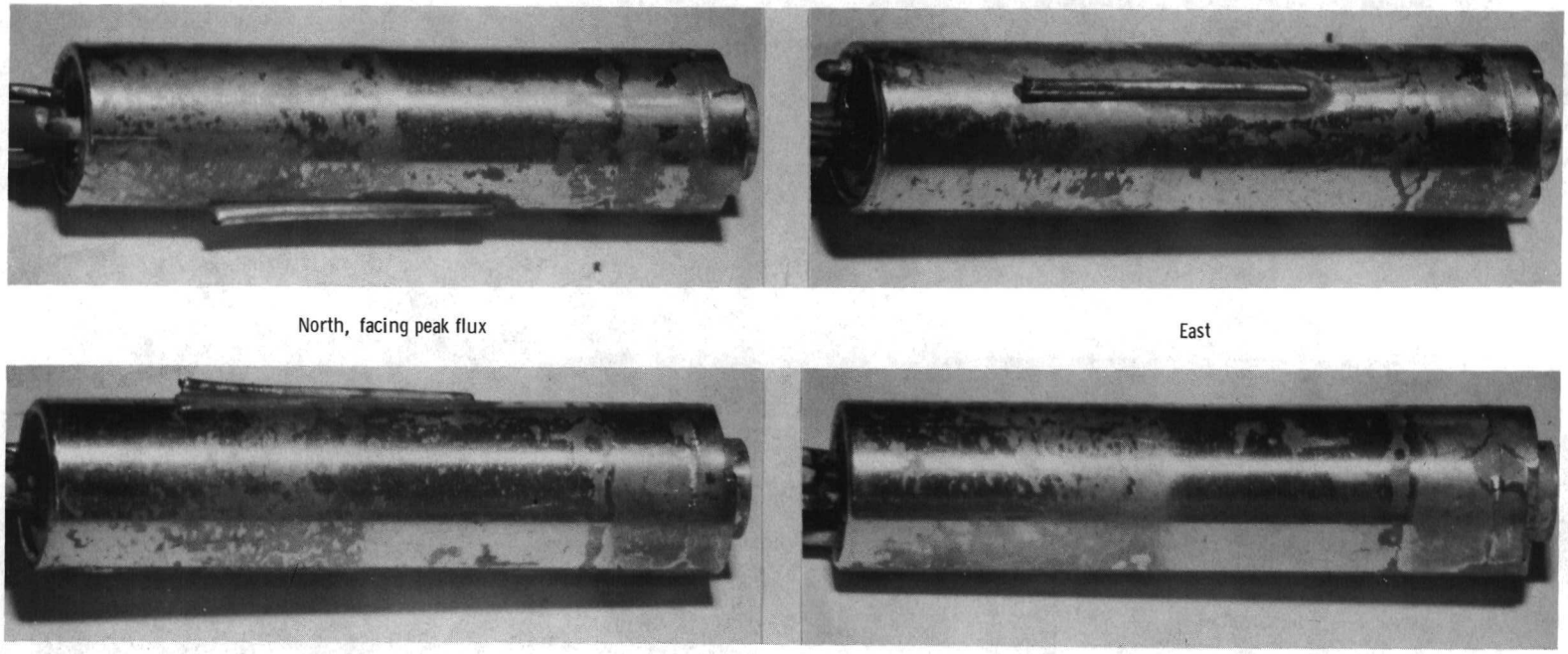

North, facing peak flux

East

South

West

Figure 17. - Steel capsule containing fuel specimen number 2 viewed from four directions. Note bright center section where fuel is located.

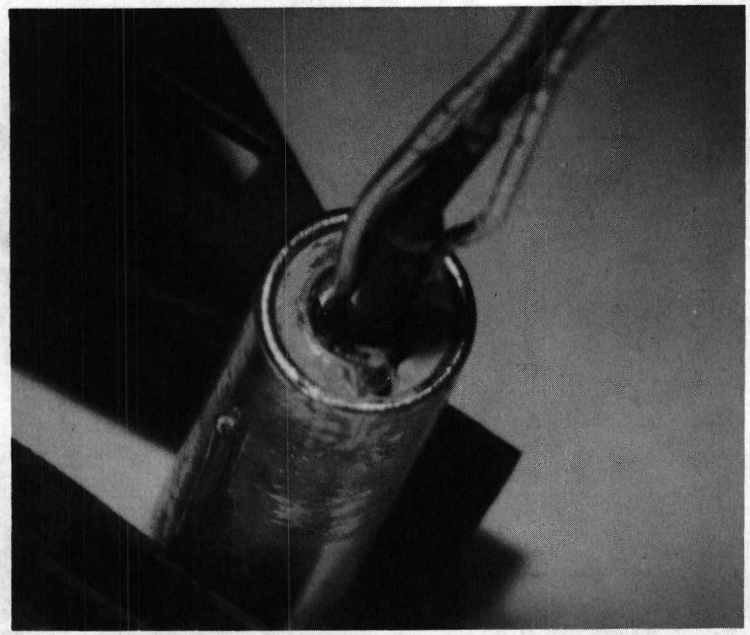

Figure 18. - Top end of steel capsule number 2 showing nickel-manganese braze around thermocouples.

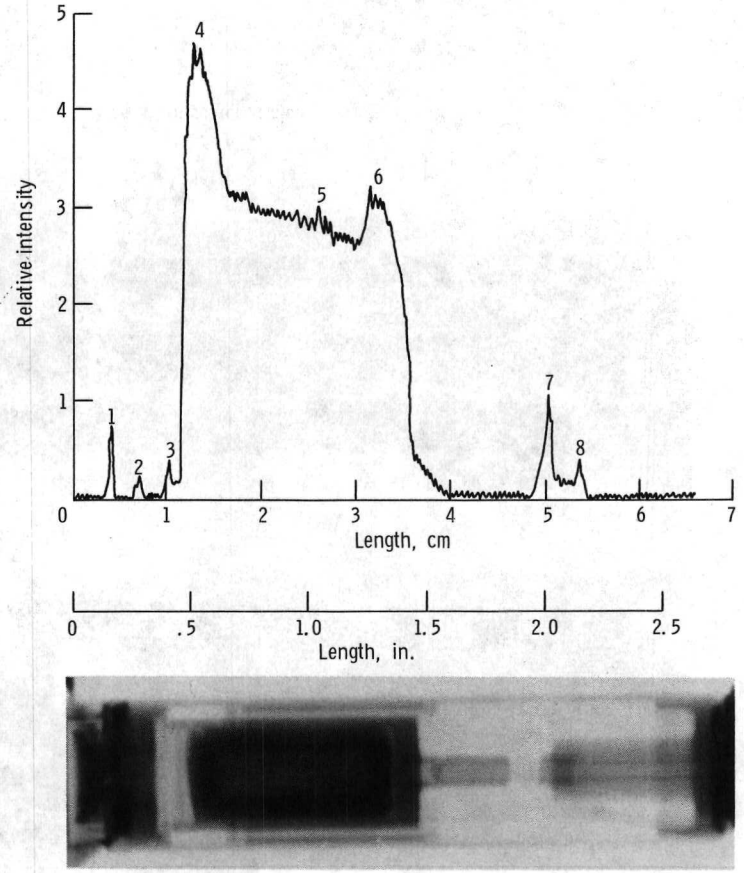

Figure 19. - Gross gamma scan of capsule plotted in relation to neutron radiograph of fuel specimen and steel container.

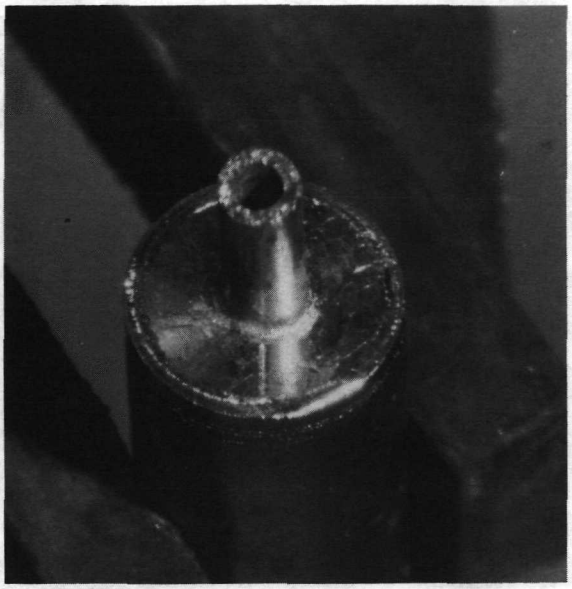

Broken stem at top of fuel specimen

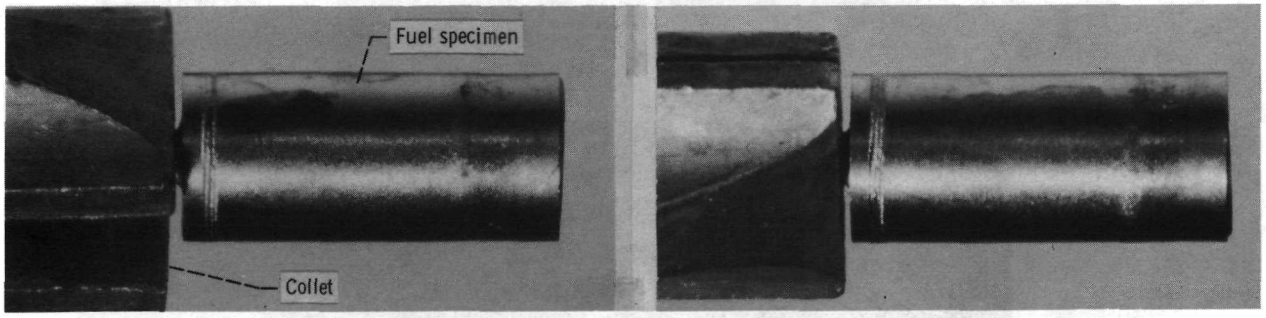

North (peak flux)

East

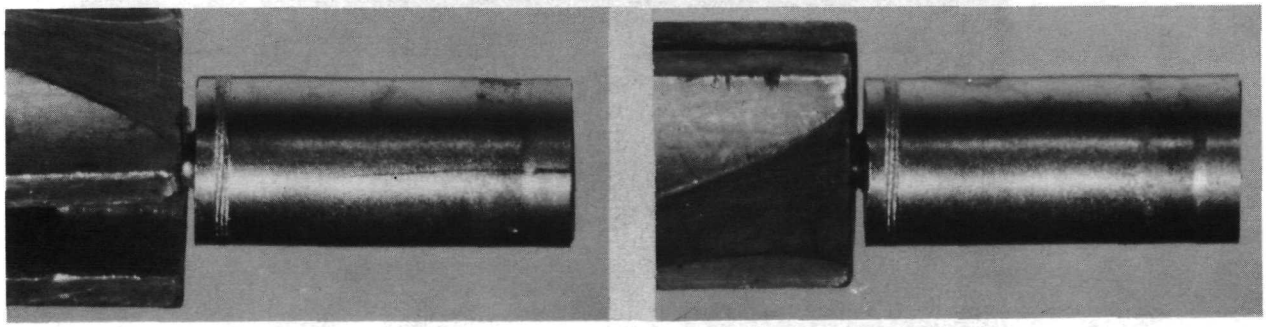

South

West

Figure 20. - Tungsten clad fuel specimen number 2 veiwed from top and four sides. No defects in cladding surface were visible. Slight diametral swelling can be seen.

Figure 21. - Remains of niobium heat sheilds stuck to bottom of fuel specimen.

Figure 22. - Top section of steel container showing crystalline deposit on walls and on thermocouple stem. Gamma scan activity peaks indicated that deposit contained solid fission products.

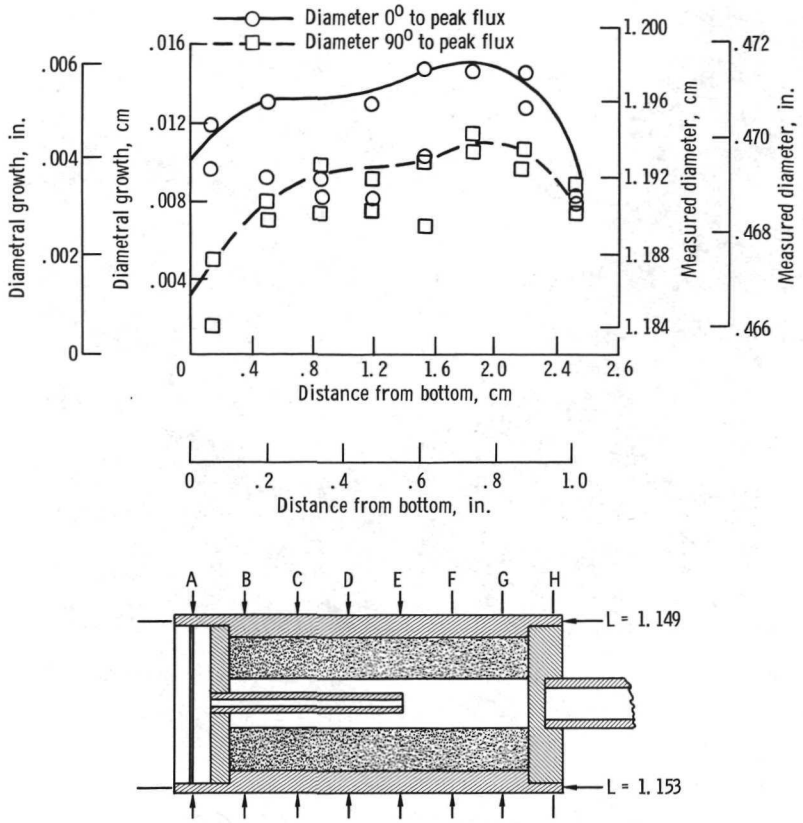

Figure 23. - Diametral change in cladding as measured at eight points longitudinally and at 0° and 90° to peak flux.

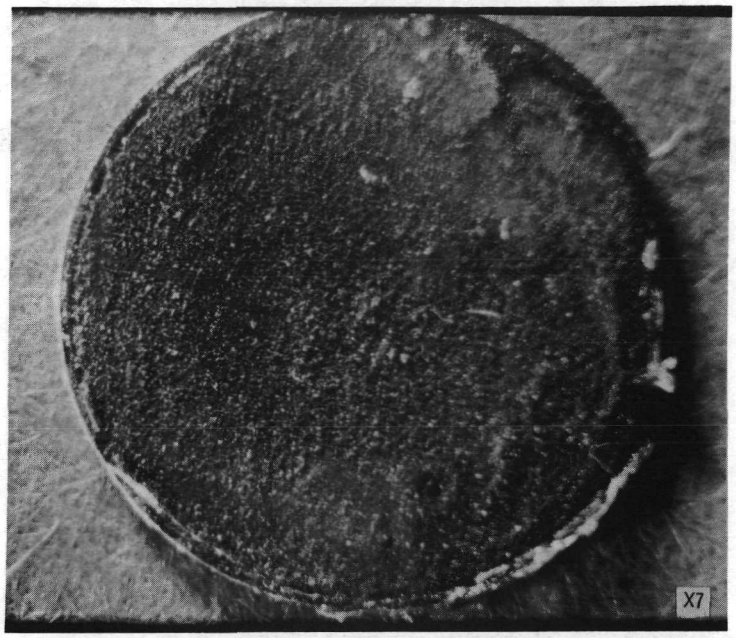

Figure 24. - Inner surface of niobium catcher plate showing deposit of uranium dioxide from vent tube and from end cap ruptured joint.

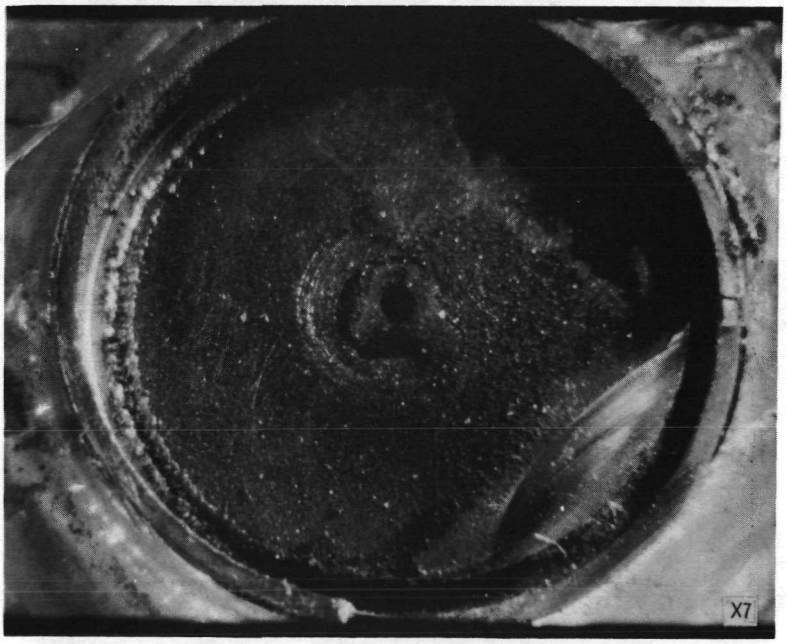

Figure 25. - Bottom end cap showing central vent tube, rupture of weld in lower right quadrant, and uranium dioxide deposit on surface. Side of specimen that faced peak flux is at top of photo. Note: scarred area at lower right was caused by false start of cutting wheel.

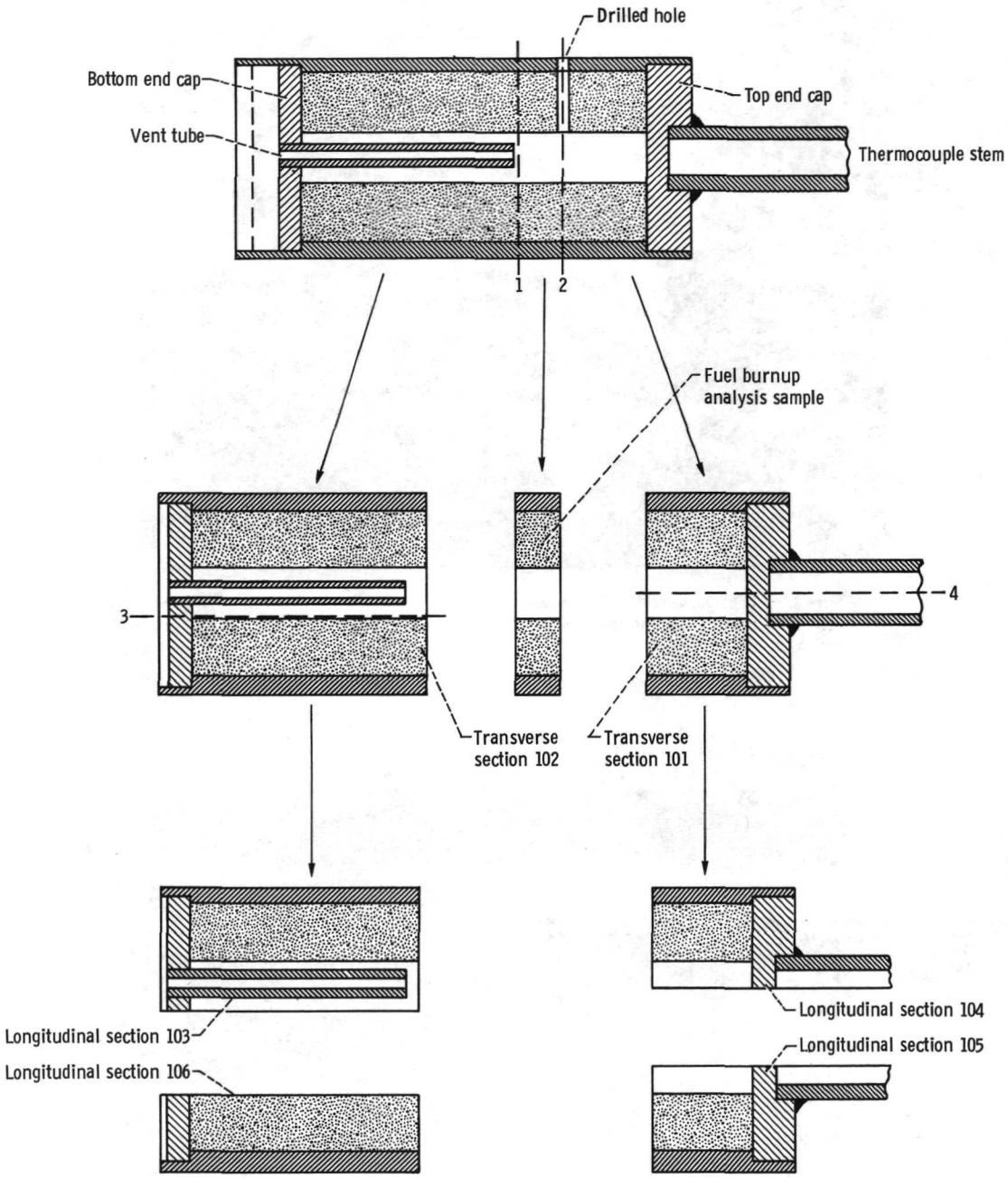

Figure 26. - Schematic diagrams of cutting of fuel specimen to provide transverse and longitudinal sections for metallographic examination.

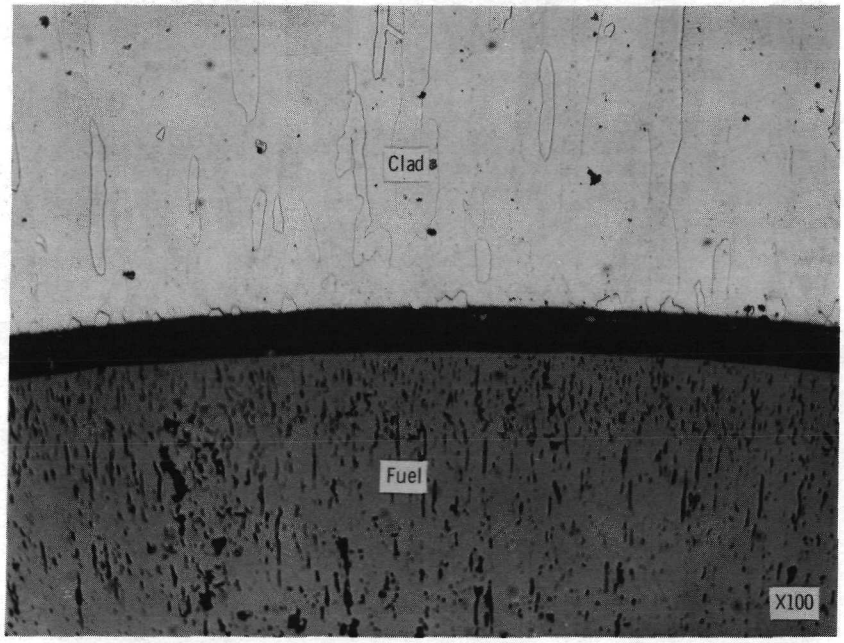

Figure 27. - Transverse section 101 showing upper half of fuel specimen, chemically vapor deposited tungsten cladding and uranium dioxide fuel pellet with no evidence of gross interaction between fuel and cladding.

Outside surface; transverse

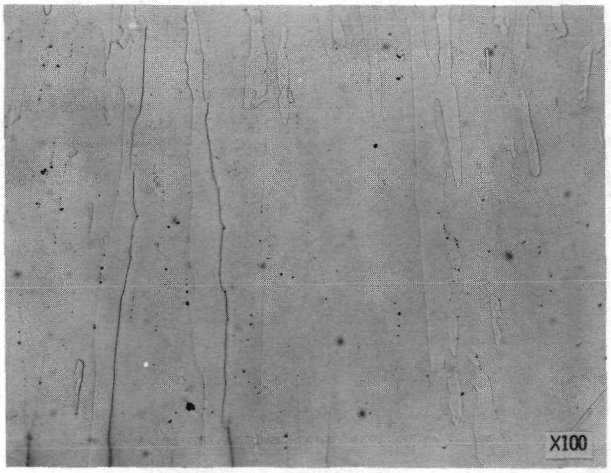

Midsection of cladding; transverse

Figure 28. - Microstructure of chemically vapor deposited tungsten cladding near top of fuel specimen, showing retention of original columnar grain structure. (Reduced 26 percent in printing.)

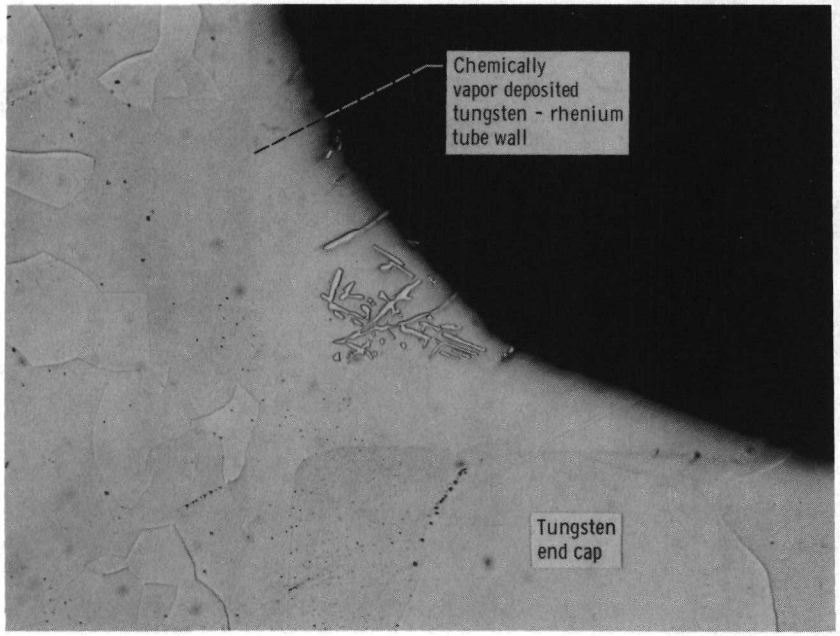

Figure 29. - Microstructure of joint between chemically vapor deposited tungsten - rhenium stem tube and arc-cast tungsten end cap, made with molybdenum - 50-weight-percent rhenium braze. Note sigma phase in braze.

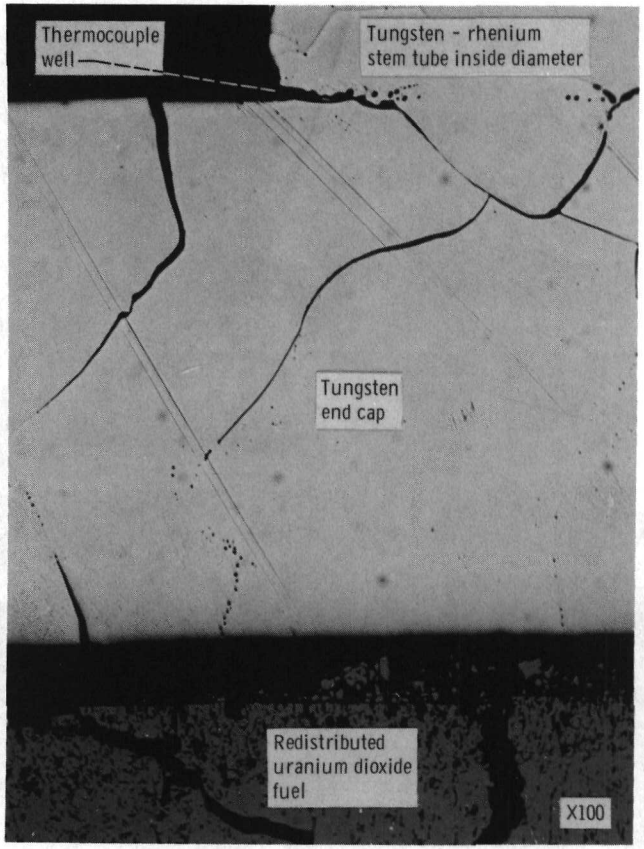

Figure 30. - Center portion of arc-cast tungsten end cap at thermocouple well showing intergranular cracking of tungsten.

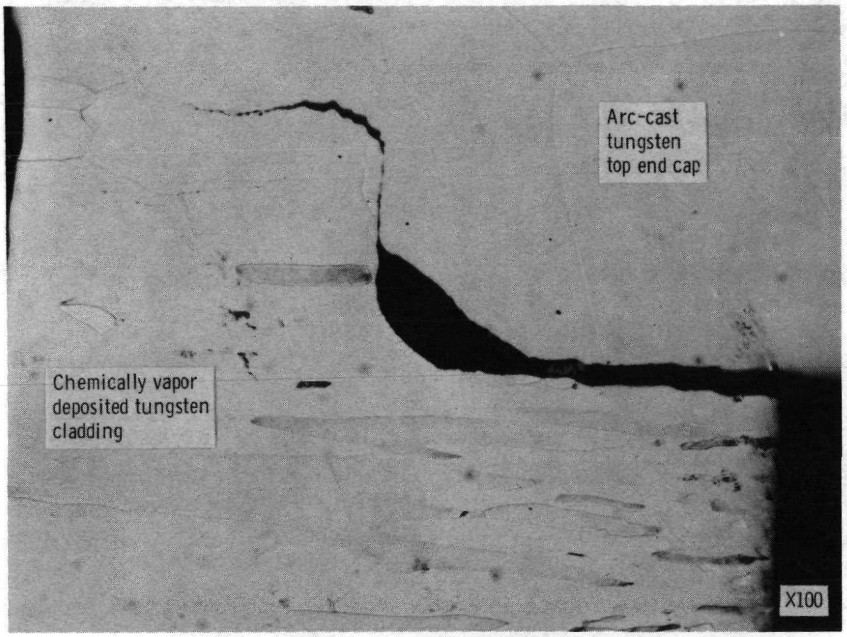

Figure 31. - Electron-beam welded joint of arc-cast tungsten top end cap to chemically vapor deposited tungsten (CVD W) cladding sleeve. Note crack propagation in grain boundary of CVD W wall at location of electron-beam spike weld.

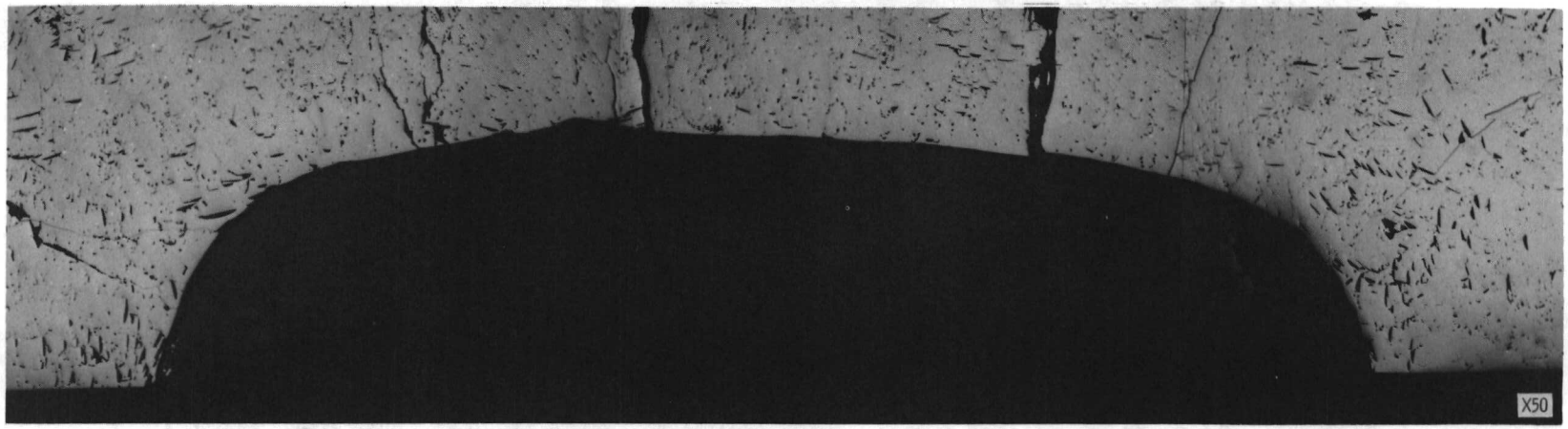

Figure 32. - Microstructure of redistributed uranium oxide fuel under top end cap of clad fuel specimen. Original fuel pellet form is shown on either side (longitudinal section). (Reduced 22 percent in printing.)

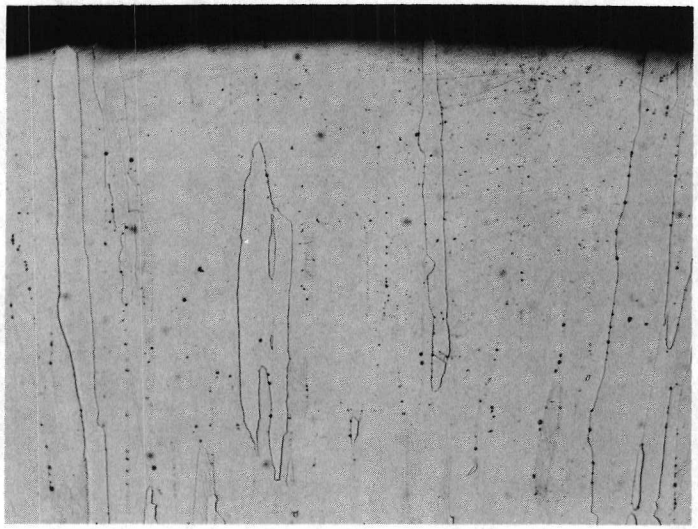

(a) Microstructure of chemically vapor deposited tungsten cladding near midsection of fuel specimen.

(b) Crack shown through cladding wall was only defect observed in transverse section.

Figure 33. - Tungsten microstructure.

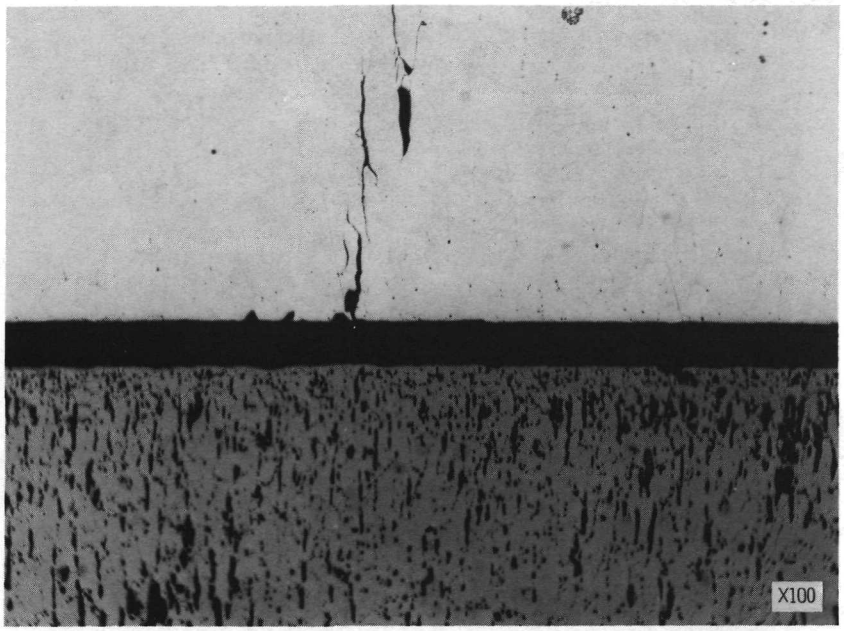

Figure 34. - Longitudinal section of fuel-cladding interface in lower portion showing intergranular cracking in chemically vapor deposited tungsten cladding.

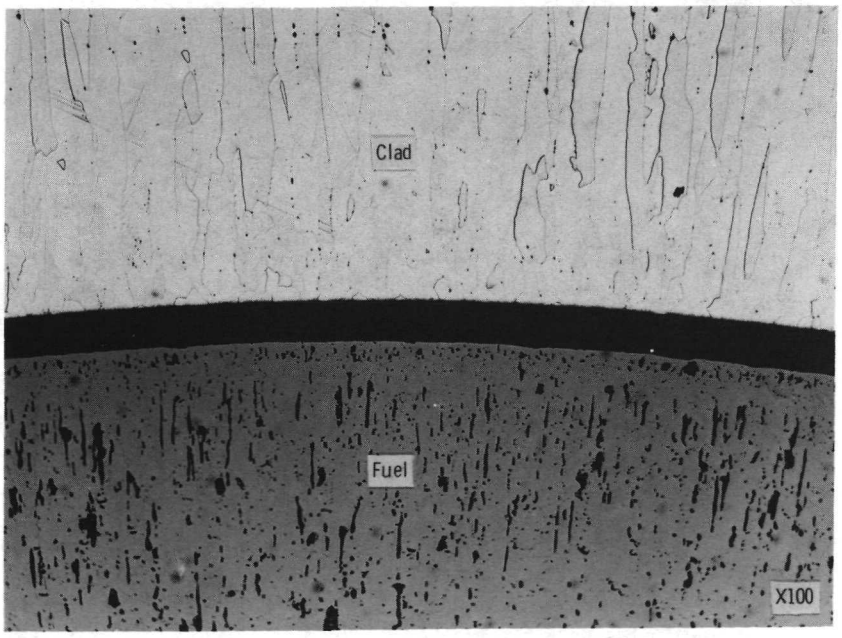

Figure 35. - Fuel cladding interface at midsection in transverse section.

Figure 36. - Montage of transverse section of redistributed uranium dioxide fuel at midsection of fuel specimen. Calculated isotherm temperature in fuel cavity during irradiation, 2250° C. (Reduced 22 percent in printing.)

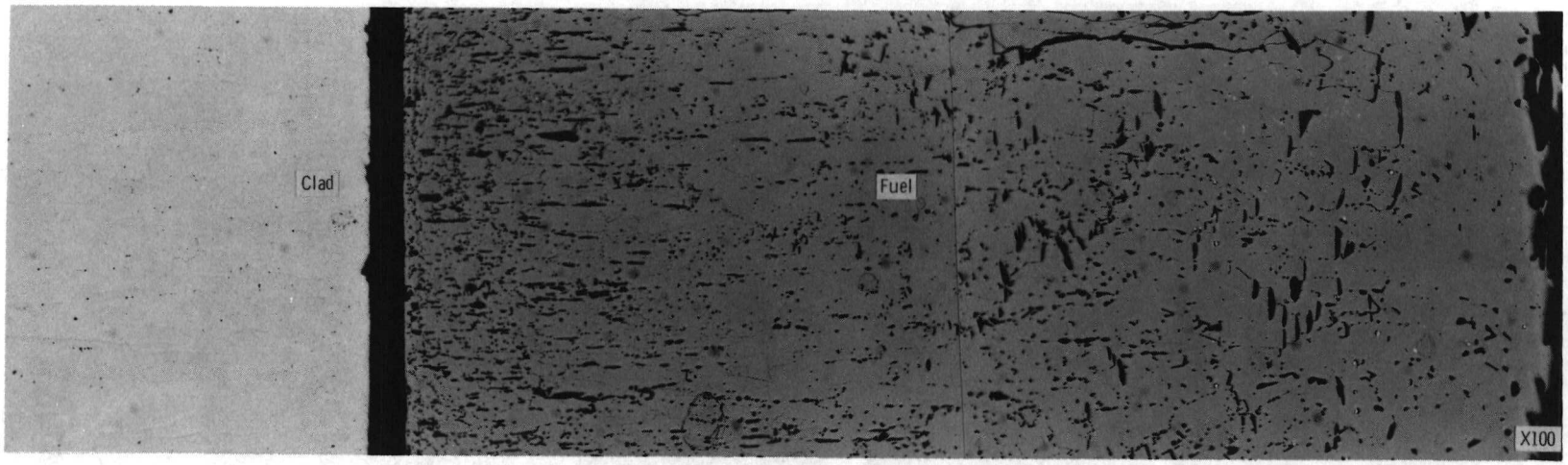

Figure 37. - Montage of longitudinal section of redistributed fuel and chemically vapor depositied tungsten cladding in lower portion of fuel specimen. Note bright metallic phase in fuel near cavity. *(Reduced 22 percent in printing.)*

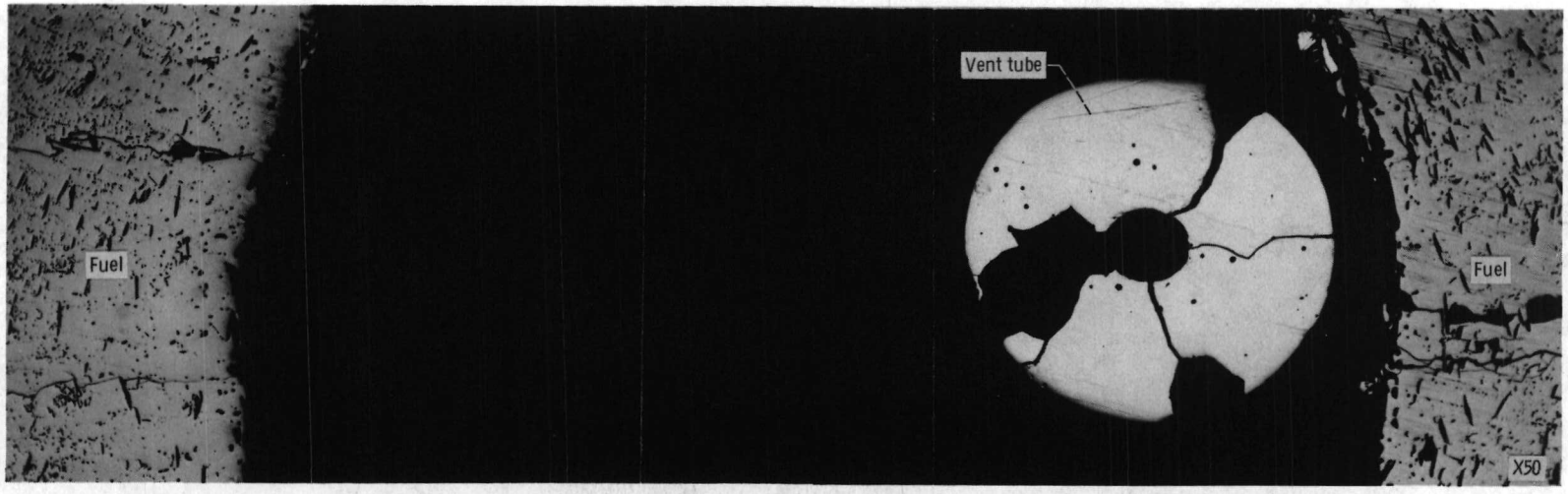

Figure 38. - Montage of transverse section 102 of fuel cavity and tip of vent tube at the specimen midsection. Vent tube was broken off at bottom end cap and lay on wall of fuel cavity. (Reduced 22 percent in printing.)

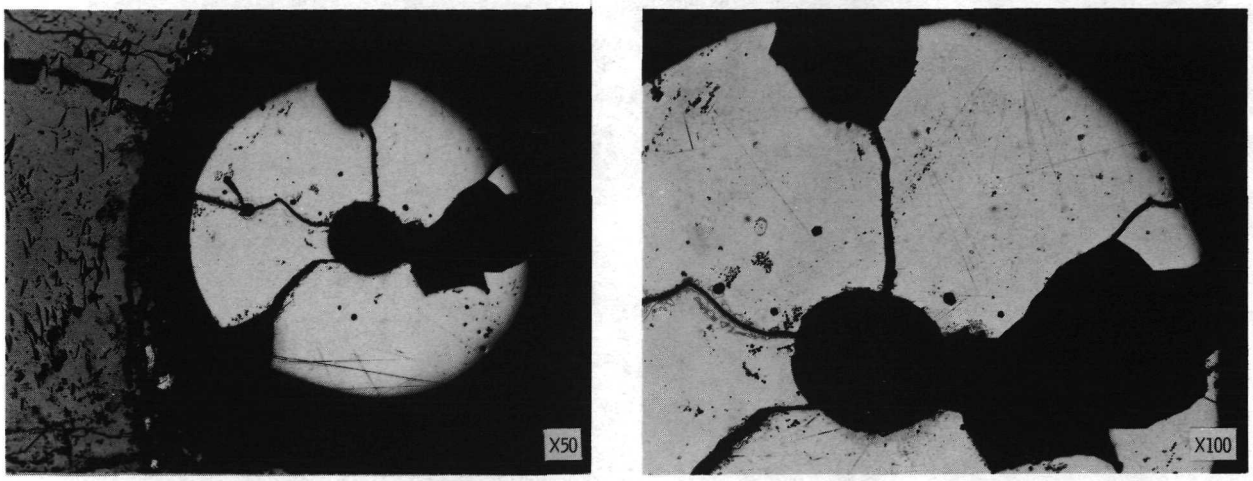

Figure 39. - End of central vent tube near midsection of fuel specimen showing chemically vapor deposited tungsten (CVD W) tube in cracked condition. Large grain growth of CVD W indicated operating temperatures greater than 2200° C.

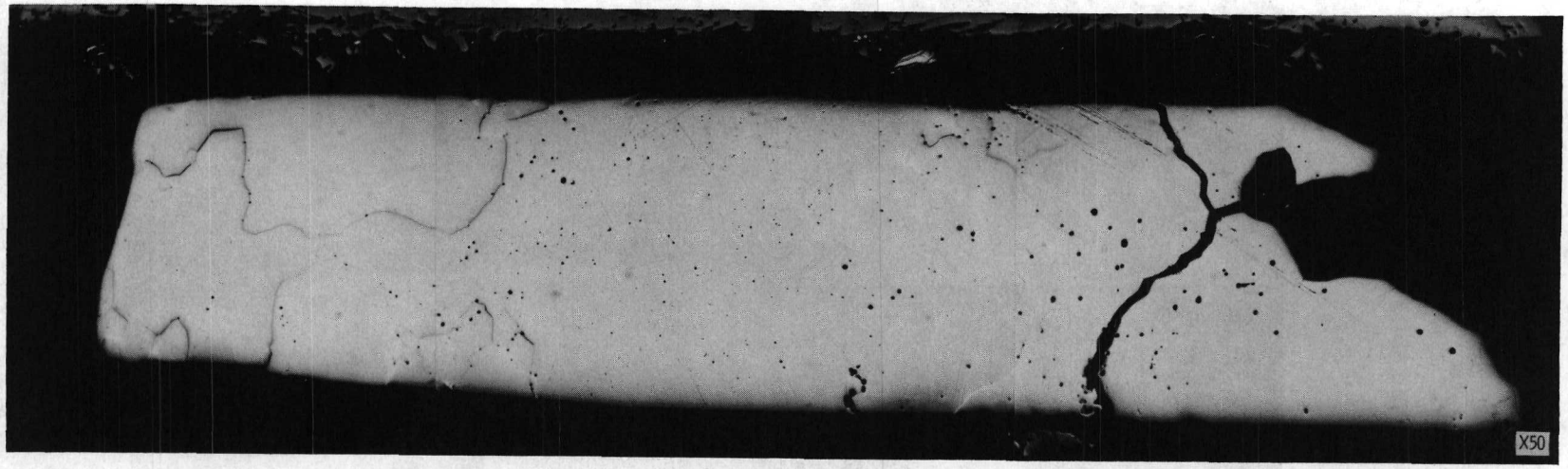

Figure 40. - Montage of longitudinal section of broken vent tube at first stage of grinding before penetrating into the 0.025-centimeter (0.010-in.) center hole. Note: Less than half the original length of 1.19 centimeters (0.47 in.) remains intact, indicating that the top end was broken off. (Reduced 22 percent in printing.)

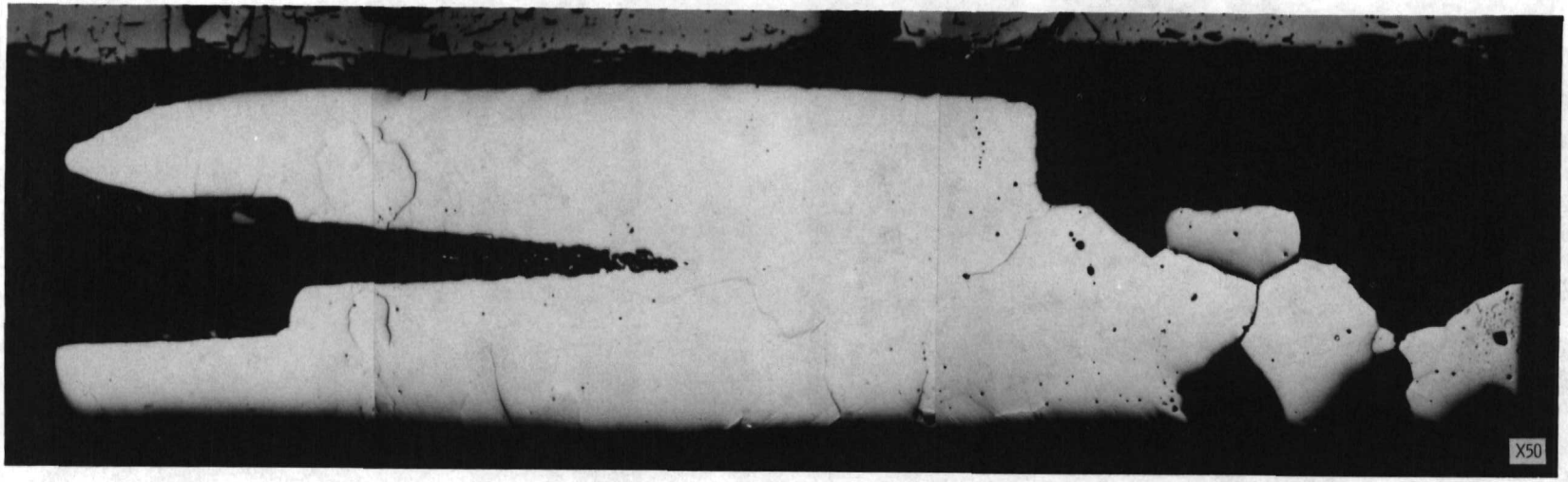

Figure 41. - Montage of longitudinal section of vent tube after second stage of grinding into center hole. Top end was broken off and bottom end with counterbore parted from bottom end cap.

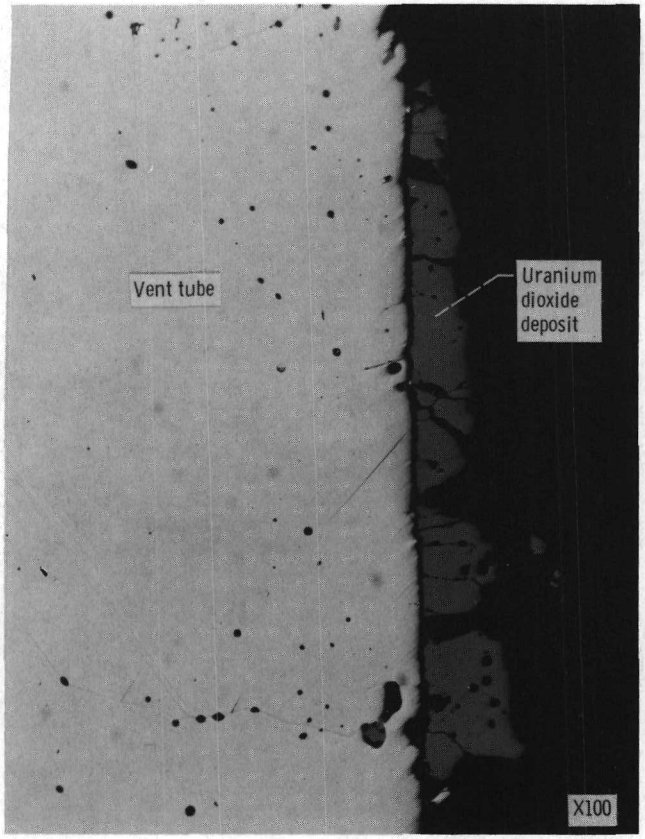

Figure 42. - Redistributed uranium dioxide deposited on outside diameter of vent tube.

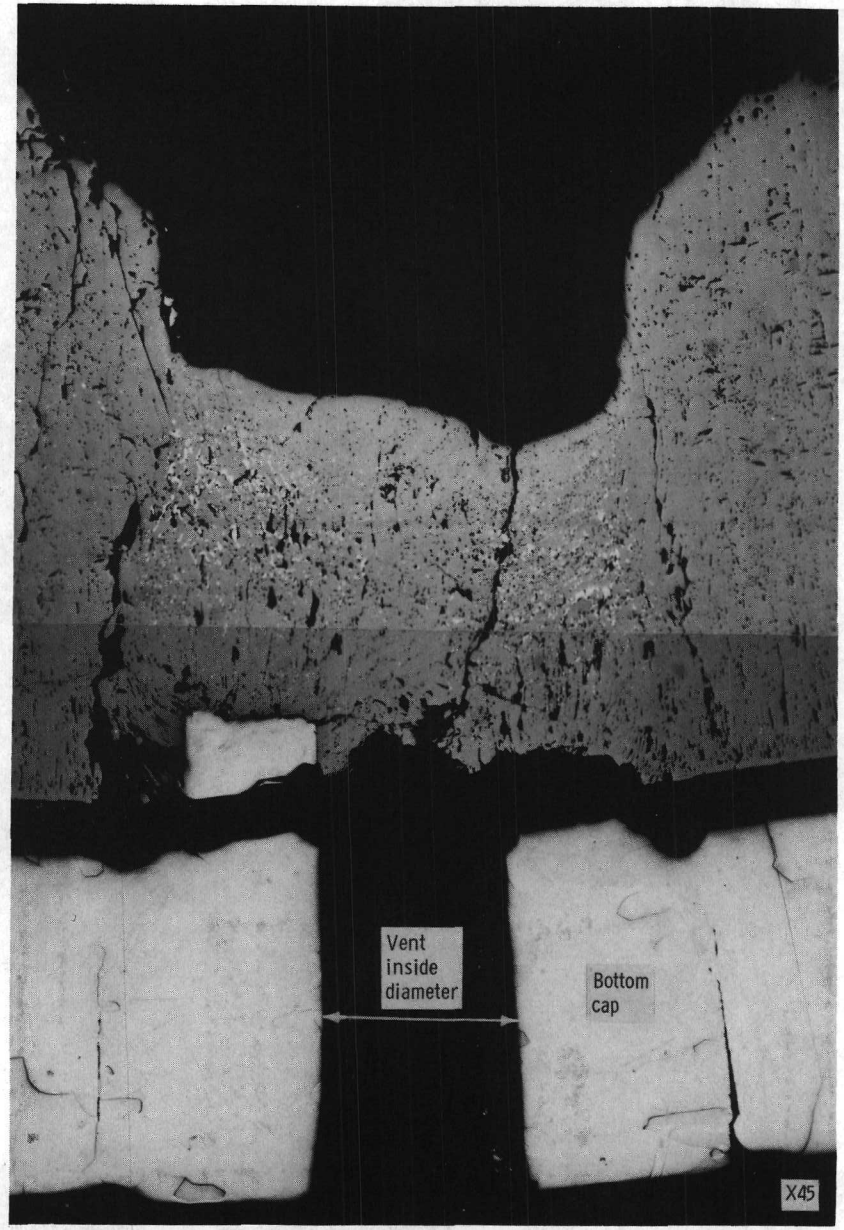

Figure 43. - Bottom end cap with base of vent tube and redistributed fuel bridging the gap where vent tube was before fracture. Note second phase in redistributed uranium dioxide.

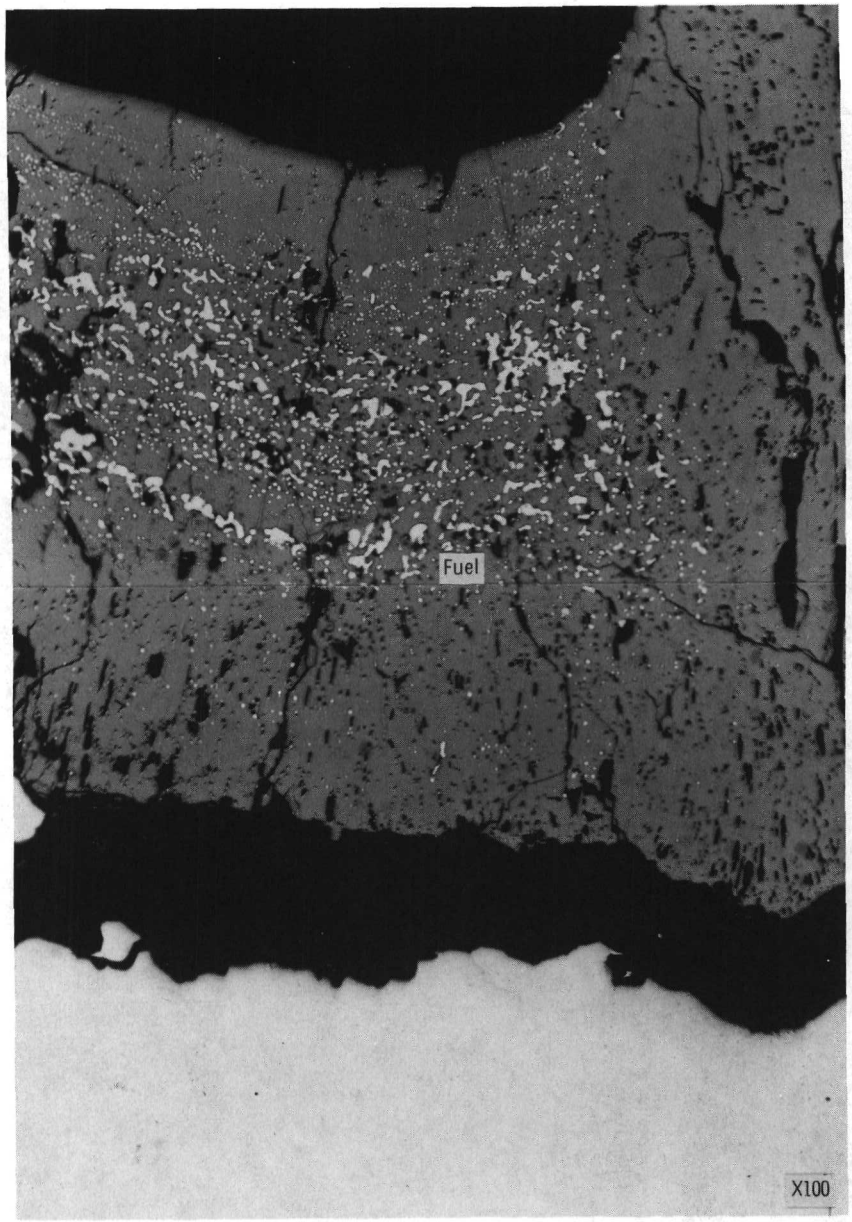

Figure 44. - Redistributed uranium dioxide at bottom end cap near central vent. Second phase in fuel (white areas) contains tungsten, iron, and nickel.

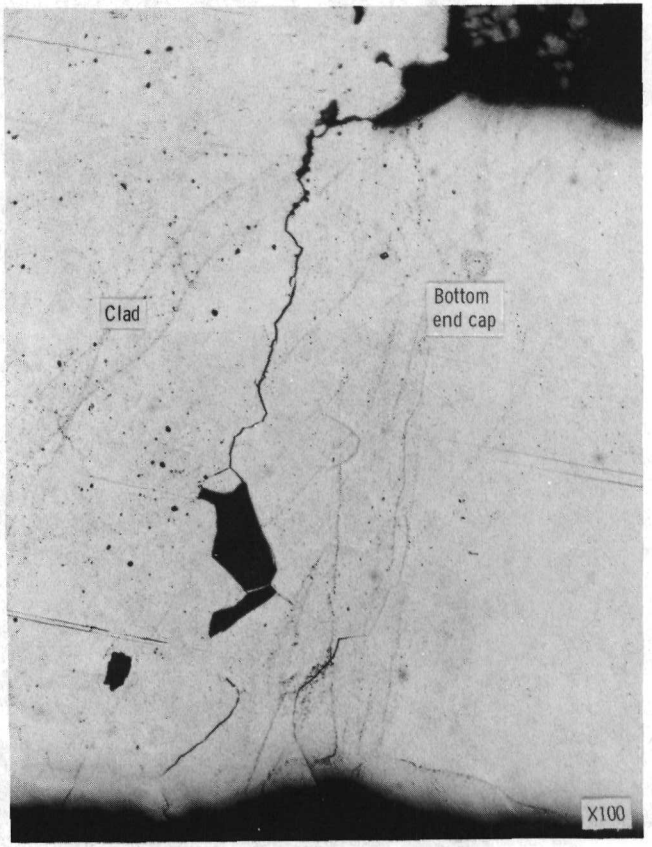

Figure 45. - Electron-beam welded joint at bottom of specimen on side opposite the rupture of end cap weld showing initiation of crack in weld joint.

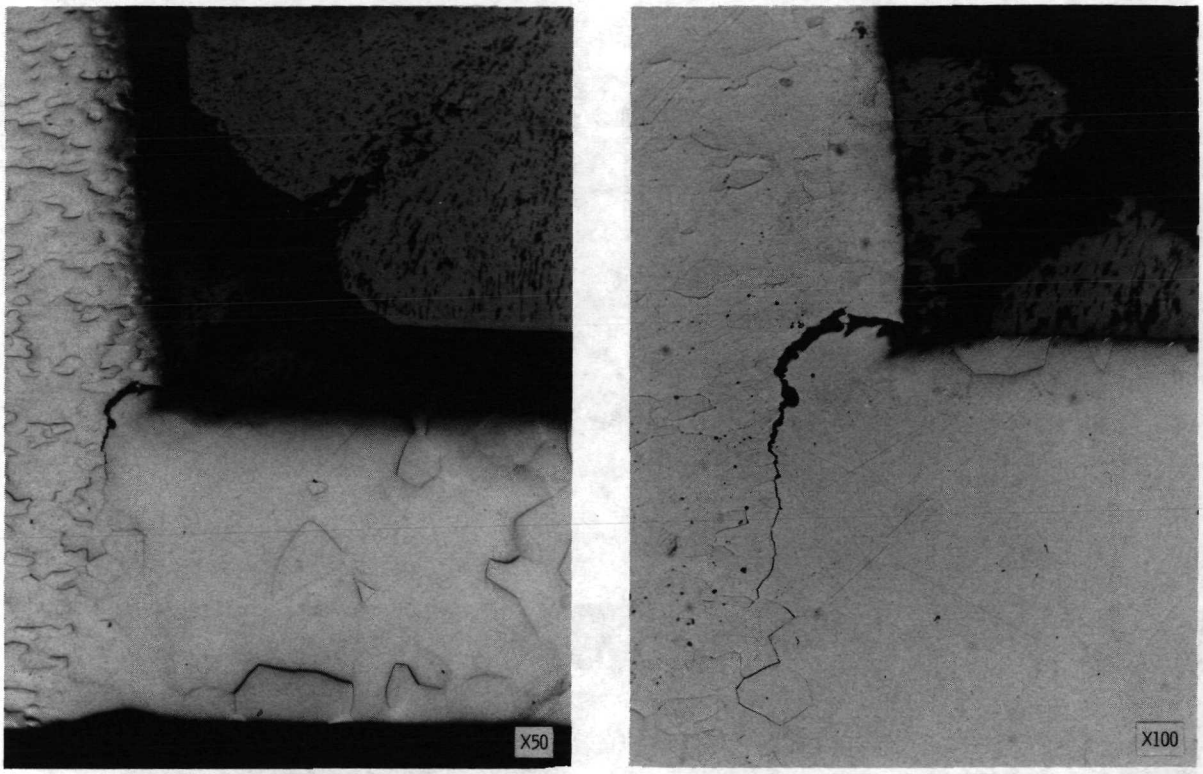

Figure 46. - Section of electron-beam welded joint between chemically vapor deposited tungsten cladding and arc-cast tungsten end cap on side opposite failure showing initiation of cracking from inside corner. (Reduced 8 percent in printing.)

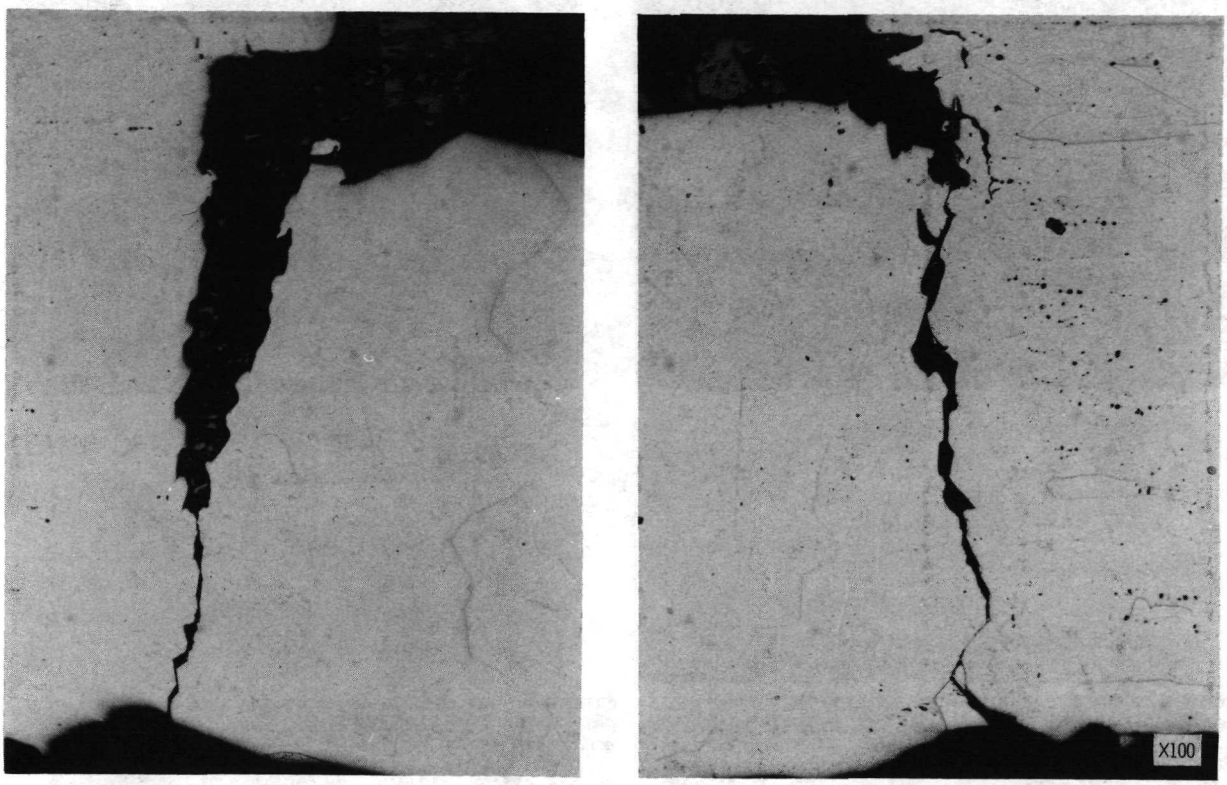

Figure 47. - Ruptured weld joint between bottom end cap and cladding sleeve. End cap was arc-cast tungsten and cladding was chemically vapor deposited tungsten. (Reduced 8 percent in printing.)

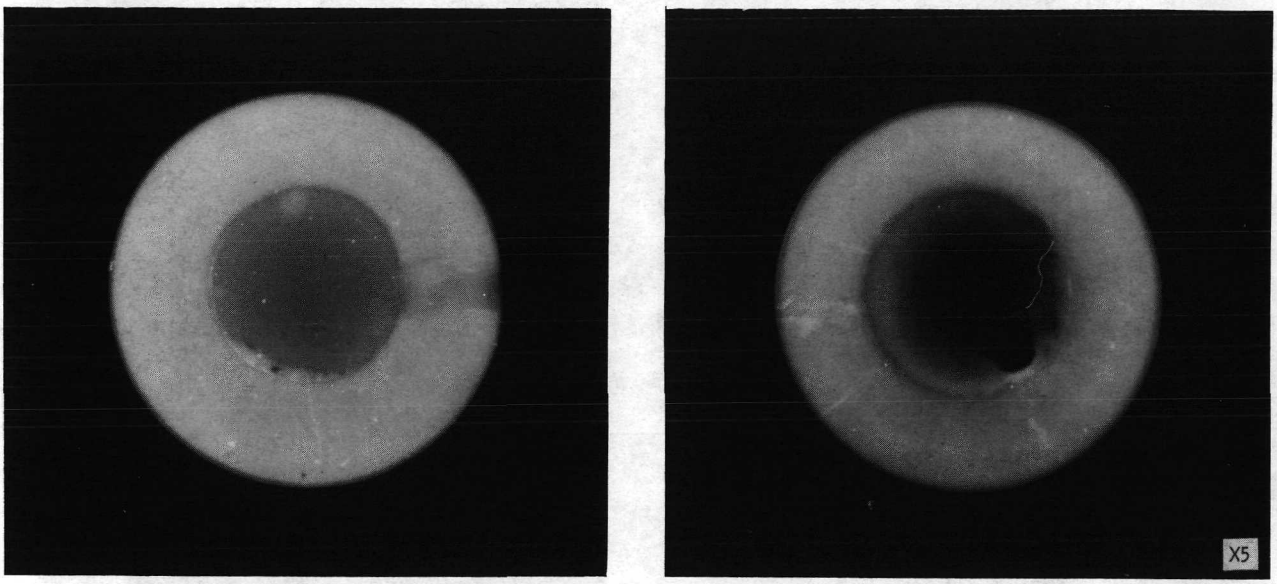

(a) Top section. (b) Bottom section.

Figure 48. - Gamma autoradiographs of transverse section of fuel specimen showing minor radial burnup gradient. Note broken vent tube on one side of cavity in bottom section and radial cracks in fuel pellet. Hole drilled through wall in top section shows as darker area.

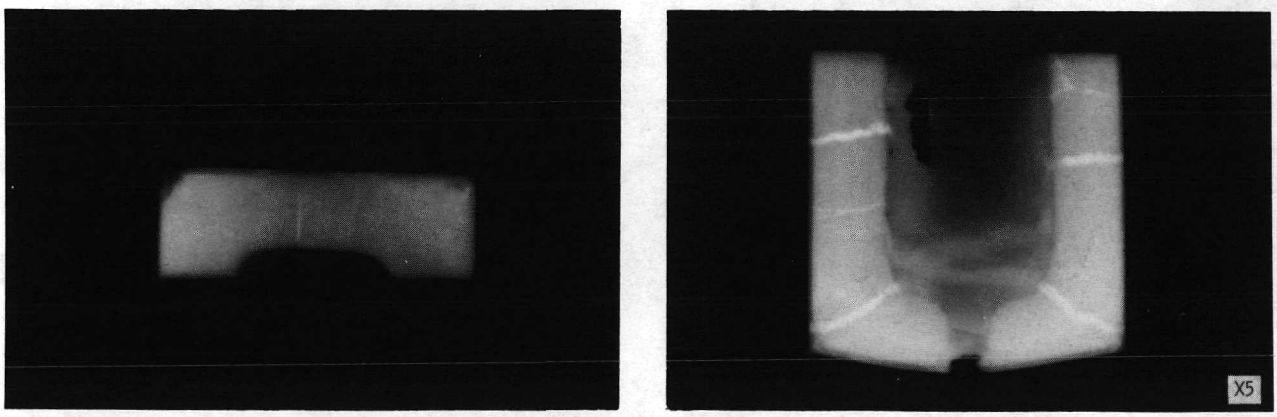

(a) Top section. (b) Bottom section.

Figure 49. - Gamma autoradiographs of longitudinal section of fuel specimen showing radial burnup gradient. Note bowed bottom end cap and remains of broken vent tube.

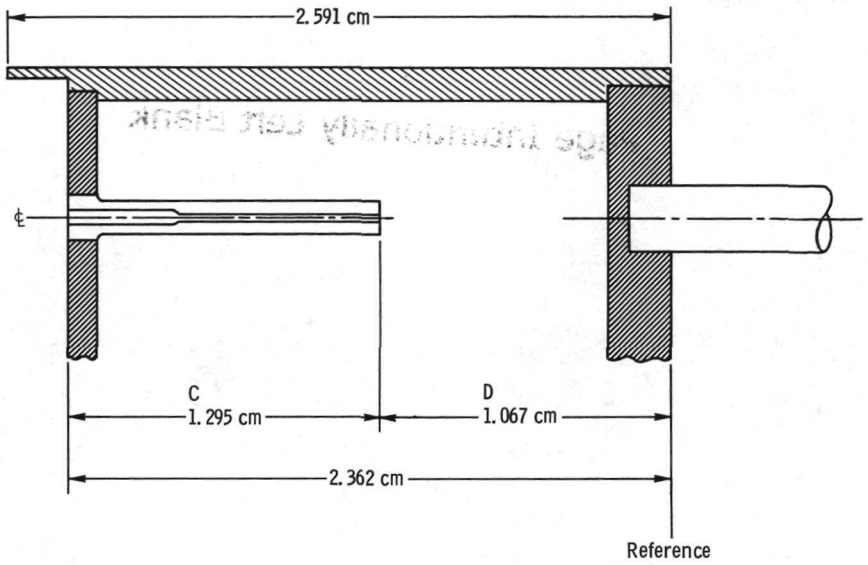

Time at temperature, hr	D, cm	C, cm	D + C, cm
191	1.100	1.260	2.380
410	1.105	1.240	2.345
410	1.105	1.234	2.339
634	1.097	1.267	2.364
1554	1.090	1.290	2.380
2607	1.118	1.308	2.426
2607	1.113	1.346	2.459
2607	1.113	1.359	2.472

Figure 50. - Vent tube motion as measured from radiograph enlargements.

Page Intentionally Left Blank

NATIONAL AERONAUTICS AND SPACE ADMINISTRATION
WASHINGTON, D.C. 20546

OFFICIAL BUSINESS
PENALTY FOR PRIVATE USE $300

SPECIAL FOURTH-CLASS RATE
BOOK

POSTAGE AND FEES PAID
NATIONAL AERONAUTICS AND
SPACE ADMINISTRATION
451

U.S.MAIL

POSTMASTER : If Undeliverable (Section 158 Postal Manual) Do Not Return

"The aeronautical and space activities of the United States shall be conducted so as to contribute . . . to the expansion of human knowledge of phenomena in the atmosphere and space. The Administration shall provide for the widest practicable and appropriate dissemination of information concerning its activities and the results thereof."

—NATIONAL AERONAUTICS AND SPACE ACT OF 1958

NASA SCIENTIFIC AND TECHNICAL PUBLICATIONS

TECHNICAL REPORTS: Scientific and technical information considered important, complete, and a lasting contribution to existing knowledge.

TECHNICAL NOTES: Information less broad in scope but nevertheless of importance as a contribution to existing knowledge.

TECHNICAL MEMORANDUMS: Information receiving limited distribution because of preliminary data, security classification, or other reasons. Also includes conference proceedings with either limited or unlimited distribution.

CONTRACTOR REPORTS: Scientific and technical information generated under a NASA contract or grant and considered an important contribution to existing knowledge.

TECHNICAL TRANSLATIONS: Information published in a foreign language considered to merit NASA distribution in English.

SPECIAL PUBLICATIONS: Information derived from or of value to NASA activities. Publications include final reports of major projects, monographs, data compilations, handbooks, sourcebooks, and special bibliographies.

TECHNOLOGY UTILIZATION PUBLICATIONS: Information on technology used by NASA that may be of particular interest in commercial and other non-aerospace applications. Publications include Tech Briefs, Technology Utilization Reports and Technology Surveys.

Details on the availability of these publications may be obtained from:

SCIENTIFIC AND TECHNICAL INFORMATION OFFICE

NATIONAL AERONAUTICS AND SPACE ADMINISTRATION

Washington, D.C. 20546